AD-A176 337 THE POLAR BEAR IONOSPHERIC EXPERIMENTS A PRE-LAUNCH OVERVIEW(U) PHYSICAL DYNAMICS INC BELLEVUE WA E J FREMOUW 09 MAY 86 PD-NW-86-144R DNA-TR-86-156 1/1

UNCLASSIFIED DNA001-85-C-0017 F/G 4/1 NL

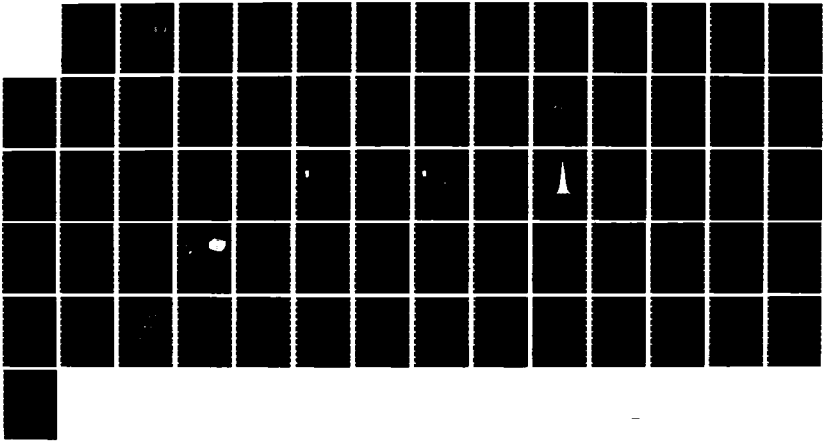

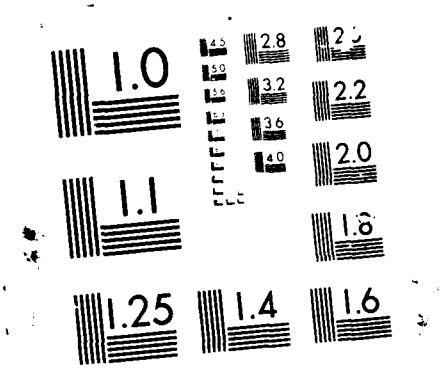
1.0
1.1
1.25
1.4
1.6
2.8
3.2
3.6
4.0
2.2
2.0
1.8

DNA-TR-86-156

THE POLAR BEAR IONOSPHERIC EXPERIMENTS

A Pre-Launch Overview

Edward J. Fremouw
Physical Dynamics, Inc.
P. O. Box 3027
Bellevue, WA 98009-3027

9 May 1986

Technical Report

CONTRACT No. DNA 001-85-C-0017

THIS WORK WAS SPONSORED BY THE DEFENSE NUCLEAR AGENCY
UNDER RDT&E RMSS CODE B322085466 I25AMXI000122 H2590D.

Prepared for
Director
DEFENSE NUCLEAR AGENCY
Washington, DC 20305-1000

DISTRIBUTION LIST UPDATE

This mailer is provided to enable DNA to maintain current distribution lists for reports. We would appreciate your providing the requested information.

- ☐ Add the individual listed to your distribution list.
- ☐ Delete the cited organization/individual.
- ☐ Change of address.

NAME: _____

ORGANIZATION: _____

OLD ADDRESS	CURRENT ADDRESS
_____	_____
_____	_____
_____	_____

TELEPHONE NUMBER: (___) _____

SUBJECT AREA(s) OF INTEREST:

_____	_____
_____	_____
_____	_____

DNA OR OTHER GOVERNMENT CONTRACT NUMBER: _____

CERTIFICATION OF NEED-TO-KNOW BY GOVERNMENT SPONSOR (if other than DNA):

SPONSORING ORGANIZATION: _____

CONTRACTING OFFICER OR REPRESENTATIVE: _____

SIGNATURE: _____

Director
Defense Nuclear Agency
ATTN: STTI
Washington, DC 20305-1000

Director
Defense Nuclear Agency
ATTN: STTI
Washington, DC 20305-1000

UNCLASSIFIED
SECURITY CLASSIFICATION OF THIS PAGE

REPORT DOCUMENTATION PAGE

Form Approved
OMB No 0704 0188
Exp Date Jun 30 1986

1a REPORT SECURITY CLASSIFICATION Unclassified	1b RESTRICTIVE MARKINGS
2a SECURITY CLASSIFICATION AUTHORITY N/A since Unclassified	3 DISTRIBUTION/AVAILABILITY OF REPORT Approved for public release; distribution is unlimited.
2b DECLASSIFICATION/DOWNGRADING EDULE N/A since Unclassified	
4 PERFORMING ORGANIZATION REPORT NUMBER(S) PD-NW-86-344R	5 MONITORING ORGANIZATION REPORT NUMBER(S) DNA-TR-86-156
6a NAME OF PERFORMING ORGANIZATION PHYSICAL DYNAMICS, INC. 6b OFFICE SYMBOL (If applicable)	7a NAME OF MONITORING ORGANIZATION Director Defense Nuclear Agency
6c ADDRESS (City, State, and ZIP Code) P.O. Box 3027 Bellevue, WA 98009-3027	7b ADDRESS (City, State, and ZIP Code) Washington, DC 20305-1000
8a NAME OF FUNDING/SPONSORING ORGANIZATION 8b OFFICE SYMBOL (If applicable)	9 PROCUREMENT INSTRUMENT IDENTIFICATION NUMBER DNA 001-85-C-0017
8c ADDRESS (City, State, and ZIP Code)	10 SOURCE OF FUNDING NUMBERS

PROGRAM ELEMENT NO	PROJECT NO	TASK NO	WORK UNIT ACCESSION NO
62715H	I25AMXI	0	DH008620

11 TITLE (Include Security Classification)
THE POLAR BEAR IONOSPHERIC EXPERIMENTS—A Pre-Launch Overview

12 PERSONAL AUTHOR(S)
Fremouw, Edward J.

13a TYPE OF REPORT	13b TIME COVERED	14 DATE OF REPORT (Year, Month, Day)	15 PAGE COUNT
Technical Report	FROM 850301 TO 851031	860509	

16 SUPPLEMENTARY NOTATION
This work was sponsored by the Defense Nuclear Agency under RDT&E RMSS Code B322085466 I25AMXI000122 H2590D.

17 COSATI CODES			18 SUBJECT TERMS (Continue on reverse if necessary and identify by block number)
FIELD	GROUP	SUB-GROUP	Radiowave Scintillation; Ultraviolet Backgrounds; High-latitude Ionosphere; Plasma-density Irregularities; Satellite Observations; High-altitude Nuclear Effects
18	2		
20	8		

19 ABSTRACT (Continue on reverse if necessary and identify by block number)

The Defense Nuclear Agency (DNA) researches nuclear weapons effects at all atmospheric levels. Given sustained success of the Limited Nuclear Test Ban Treaty, understanding such atmospheric effects is achieved by extrapolating fundamental knowledge about the atmosphere and its dynamics. In the current era of intense interest in space-based systems, stemming in large part from the Strategic Defense Initiative, questions about High-Altitude Nuclear Effects (HANE) are receiving particular attention. A central issue in DNA's HANE research program for some time has been the development of striations and other structures in plasmas convecting through the high-altitude neutral atmosphere under the influence of the earth's magnetic and electrostatic fields. Such plasma structures not only scatter radio waves, causing C^3I signals at radio frequencies to scintillate, but they also can appear as variable backgrounds to electro-optical sensors operating on infrared, optical, and ultraviolet wavelengths.

20 DISTRIBUTION/AVAILABILITY OF ABSTRACT	21 ABSTRACT SECURITY CLASSIFICATION
☐ UNCLASSIFIED/UNLIMITED ☒ SAME AS RPT ☐ DTIC USERS	UNCLASSIFIED

22a NAME OF RESPONSIBLE INDIVIDUAL	22b TELEPHONE (Include Area Code)	22c OFFICE SYMBOL
Betty L. Fox	(202) 325-7042	DNA/STTI

DD FORM 1473, 84 MAR — 83 APR edition may be used until exhausted; All other editions are obsolete

SECURITY CLASSIFICATION OF THIS PAGE
UNCLASSIFIED

19. ABSTRACT (Continued)

The DNA Wideband Satellite (P76-5) documented and diagnosed scintillation effects from VHF through S band, and its successor, HiLat (P83-1), has built on that information and other results of ionospheric research to provide considerable understanding of the dominance of convection in the development of scintillation-producing irregularities. Launched in June of 1983, HiLat's five experiments have returned valuable information on scintillation and on plasma behavior and its electrodynamic environment in the ionospheric F layer at high latitudes. Its most ambitious experiment failed, however, after providing a number of tantalizing vacuum ultraviolet images of the aurora before simultaneous scintillation observations using HiLat's multi-frequency coherent beacon commenced.

That disappointment is being remedied, and other objectives of DNA's HANE program and the ionospheric research program of the Air Force Geophysics Laboratory are being addressed, by launch of a follow-on Polar BEacon and Auroral Research (Polar BEAR) satellite, P87-1. Polar BEAR will carry three ionospheric experiments: (1) a beacon functionally identical to that on HiLat, (2) a three-axis vector magnetometer for detecting field-aligned and other currents in the ionosphere and for assisting in determination of the satellite's attitude, and (3) an improved imager, the Auroral/Ionospheric Remote Sensor (AIRS). In addition to providing images of the aurora and airglow at four visual and vacuum ultraviolet wavelengths, AIRS will function as an ultraviolet spectrophotometer. Using AIRS in its imaging mode and receiving stations in Norway, Greenland, Northwest Territories, Manitoba, and Washington state, it will be possible to obtain images of essentially the entire auroral oval in broad daylight as well as in darkness.

Polar BEAR is scheduled for launch in the fourth quarter of CY 1986 into a nearly circular orbit near 1000 km altitude and 82 inclination. That orbit will afford a broad view for AIRS and many opportunities for coordinated observations of (1) scintillation using the beacons on both HiLat and Polar BEAR, (2) major current systems flowing between the ionosphere and magnetosphere using the magnetometers on both satellites, and (3) energetic electron precipitation and ambient plasma convection at 800 km altitude as recorded with HiLat's electron spectrometer and thermal-plasma monitor. These observations and the macro-scale context provided by AIRS should contribute significantly to further understanding of plasma processes instrumental to the development of density irregularities in the highly dynamic high-latitude ionosphere.

PREFACE

The author expresses thanks to the following individuals for information and materials contributed to this report: R. Livingston and M. Cousins of SRI International, R. Huffman of the Air Force Geophysics Laboratory, and T. Potemra and D. Grant of the Johns Hopkins University Applied Physics Laboratory.

CONVERSION TABLE

1 pound (lb.) = 0.45 kilograms

1 inch (in) = 2.54 centimeters

1 foot (ft) = 0.305 meters

1 kilometer (km) = 0.62 statute mile = 0.54 nautical mile

1 angstrom (Å) = 0.1 nanometer

1 nanotesla (nt) = 10^{-9} webers/meter^2 = 1 gamma = 10^{-5} gauss

TABLE OF CONTENTS

LIST OF ILLUSTRATIONS

LIST OF TABLES

SECTION 1

INTRODUCTION

In carrying out its mission of predicting and assessing potential nuclear effects on military systems, the Defense Nuclear Agency (DNA) conducts research programs at all atmospheric levels from the surface through the ionosphere. Against the background of sustained success enjoyed by the Limited Nuclear Test Ban Treaty, refining and extending such predictions and assessments requires extrapolation from fundamental knowledge about the atmosphere and its dynamic processes. Given the established utility of space-based elements in C^3I systems and the attention presently being focused on space-based defense systems under the Strategic Defense Initiative (SDI), high-altitude nuclear effects (HANE) and their potential interaction with the ambient ionosphere are of particular current interest.

Central to DNA's HANE Program is understanding the dynamics of large plasma patches introduced into the ionosphere and subsequently acted upon by the earth's electric and magnetic fields and by winds blowing in the surrounding neutral atmosphere. Even at very late times after injection of such plasmas, their convective motions and attendant structuring can cause disruptive scintillations to C^3I systems due to radiowave scattering produced by the structures. Infrared, visual-wavelength, and ultraviolet emissions from these plasmas, from their background, and especially from structures in both also can be disruptive to electro-optical sensors and systems.

The fundamental importance of convective instabilities in generating structures that can cause radiowave scintillation and optical fluctuations has been established for some time. Important contributions to identifying the importance of such instabilities were made by the DNA research community in mid-latitude field programs of ionospheric Barium release, in detailed and sustained observations of the more dynamic but still relatively simple ambient equatorial ionosphere, and in theoretical analyses and numerical simulations of the plasma dynamics involved.

Having achieved a good deal of fundamental understanding in the aforementioned programs, DNA more recently has attacked the far more complex problem of ionospheric plasma dynamics at high latitudes. Building on the survey information returned by its single-experiment radio beacon satellite, Wideband (Rino *et al*, 1977; Fremouw *et al*, 1978), DNA has focused its ionospheric attention on those

regions between the plasmapause and the geomagnetic pole, by means of a multi-experiment satellite, HiLat (Fremouw, 1983; HiLat Science Team, 1984; Fremouw, 1985).

HiLat (P83-1) was launched into a high-inclination, circular orbit near 800 km altitude on 27 June 1983. In addition to a five-frequency, coherent radio beacon based on the ten-frequency Wideband design, it carries four other experiment packages for *in-situ* and remote sensing of the ionospheric plasma, its optical emissions, and its electromagnetic environment. While one of three sensors in one of those four experiment packages was damaged on launch, and while there have been some other instrument failures in the almost three years since HiLat's launch, its beacon remains fully operational and continues to return direct information on radiowave scintillation as well as highly useful and informative telemetry from the other healthy instruments. A brief review of HiLat's operational history and salient scientific results to date will be given in Section 3.

To further the objectives of DNA's high-latitude HANE research program, which will be sketched in Section 2, the Polar BEacon and Auroral Research (Polar BEAR) satellite, P87-1, will be launched as a companion to HiLat into a somewhat higher (1000 km) orbit at the same inclination (82°) late in 1986. While being shared with a payload not of concern here, Polar BEAR will carry three experiment packages integral to DNA's Hilat/Polar BEAR ionospheric objectives. Indeed, the three are those originally suggested by the author (Fremouw, 1980, 1981) for what became a more ambitious HiLat mission, namely a coherent beacon, a magnetometer, and an auroral imager.

The Polar BEAR Beacon, built by SRI International as a successor to its successful HiLat Beacon, will enlarge our data base on high-latitude scintillation substantially. Not only will it produce more frequent passes over existing receiving stations, but it should extend continuous observations through a substantial portion of the solar activity cycle. Of at least equal importance, since it will carry telemetry from Polar BEAR's other two instruments, it will permit coordinated imaging of the aurora and scintillation measurements.

Polar BEAR's magnetometer, being provided by Johns Hopkins University's Applied Physics Laboratory (APL), is of advanced design and will be operated in a magnetically quieter host environment than its predecessor on HiLat. Finally, the new imager not only will follow up on tantalizing nightside and dayside auroral images produced by HiLat prior to failure of its imager's power supply, but it also

will be a substantially improved instrument. It is being provided by APL and the Air Force Geophysics Laboratory (AFGL). Each of the Polar BEAR ionospheric payloads will be described in Section 4. The satellite and its orbit will be described briefly in Section 5.

The network of receiving stations established for HiLat will be employed for Polar BEAR as well, with some stations being augmented for two-satellite operation and avoidance of mutual interference. The data will be analyzed and interpreted by a team of scientists from the aforementioned organizations; Physical Dynamics, Inc.'s Northwest Division (PDNW); Mission Research Corporation (MRC); the Naval Research Laboratory (NRL); other contractors of DNA, AFGL, and NRL; and Canadian participants. Station operations and data analysis and exchange will be outlined in Section 6.

SECTION 2

OBJECTIVES

The overall objectives of DNA's HANE research program are quite broad, involving the understanding of many phenomena that would follow a nuclear burst at high altitudes and applied to many types of military systems. Those objectives served by HiLat/Polar BEAR are classified as late-time ones, when interest centers on the behavior and effects of plasma-density enhancements introduced by the explosion, when the large-scale magnetic field, $\vec{B}$, in which the plasmas reside has returned essentially to ambient, and when transients in the electric field, $\vec{E}$, have decayed to an electrostatic state.

Under the above-described late-time conditions, high-altitude plasma convects under the influence of an $\vec{E} \times \vec{B}$ force, moving through the background neutral gas, which itself may be in motion due to neutral winds produced by both the hot burst and ambient conditions. Plasma enhancements then are subject to convective instability of their associated gradients, leading to smaller-scale structures. The aggregate of plasma structures, both the convecting large-scale patches and their evolving smaller-scale substructures and striations, can disrupt C^3I systems by means of radiowave refraction and scattering, or scintillation, and spatially structured optical emissions therefrom are of concern for electro-optical sensors.

The ultimate objectives of HiLat/Polar BEAR are to provide a sound scientific basis for designing C^3I systems and electro-optical sensors that effectively will be immune from disruption by the effects of structured high-altitude plasmas and to identify effects not likely to be surmounted by design choices. Signal-statistical, propagation-theoretical, and radiative-transfer tools for doing so exist, and descriptive information on the relevant structures is being accumulated rapidly by means of HiLat. The specific objectives for which Polar BEAR is being launched will be described at the end of this section. First, we point out the HANE objectives most closely tied to high-latitude ionospheric research, which are double-edged.

The high-latitude ionospheric F layer, in both its auroral (sub-polar) and polar regimes, is replete with naturally occuring arcs, blobs, patches, and other forms of plasma enhancement. Moreover, the cross-polar-cap electric field generated by the solar wind's interaction with the earth's magnetosphere provides a

ready source of free energy for convectively transporting such features through large distances. The attendant dynamics are sufficiently closely related to those that would act on high-altitude nuclear plasmas that properly interpreted observations of the former are providing insight into the evolutionary development of the latter.

The second HANE objective of HiLat/Polar BEAR -- the back edge of the first, as it were -- has to do specifically with the high-latitude environment itself. The two-satellite program affords a context in which to formulate and probe pertinent questions that only recently have begun to be asked, questions such as: What would be the geophysical consequences of large-scale nuclear engagement at high latitudes? These tend to be macro- and global-scale questions, a pertinent one being the consequences of substantially altering the plasma content and conductivity on magnetic flux tubes extending to great altitudes and into the earth's magneto-tail.

Interpretation of data being returned from HiLat, especially when macro-scale and quasi-global images of the aurora at visual and ultraviolet wavelengths are added from Polar BEAR, should provide oportunity to begin addressing the foregoing questions. At the same time, guidance in posing the questions in an orderly and productive manner should come from global-scale ionospheric/magnetospheric modeling being intiated at NRL (Fedder *et al*, 1986) by means of numerical simulation.

Returning to the more specific objective of understanding the plasma dynamics leading to potentially disruptive density structure, several hypotheses are being explored. Prior to launch of HiLat, two broad classes of competing hypotheses were before us. First was the view that the dominant source mechanism for scintillation-producing irregularities is convective instability, proceeding independently of latitude, origin of the plasma, and other circumstances. The opposite view was that the plasma source plays a dominant role in dictating the shape and strength of the irregularities and, therefore, the specifics of scattering geometry and severity. In the ambient high-latitude ionosphere, for instance, the latter view would postulate that the spatial spectrum of scintillation-producing irregularities is laid down directly by structured particle precipitation.

To date, HiLat has presented no convincing evidence to support the latter view. Convection through the background atmosphere appears to be the dominant factor at high latitudes, just as it is near the equator and (in the appropriate

reference frame) for test plasmas artifically introduced (by means of Barium releases) into the ionosphere at middle latitudes. Moreover, the accumulating data base suggests that the irregularity spectrum and its evolution are quite independent of the specific convective driver (gravity, neutral winds, or electrostatic convection augmented by field-aligned currents). This behavior strengthens confidence in the extrapolation of crucial results from ambient observation to nuclear application.

While the irregularity spectrum appears quite universally to be well described by a power-law decay from large structures to smaller ones, there are spectral features and trends, as well as questions of three-dimensional configuration (anisotropy of the irregularities and their spectrum) still to be clarified and understood. For instance, breaks between somewhat different power-law regimes exist in both equatorial and high-latitude irregularity spectra. The nature, consistency, and variations in these breaks currently are being explored by means of spectra from HiLat, Wideband, and other satellites, and understanding their origin and behavior will be an objective in the Polar BEAR era.

Regarding three-dimensional configuration, HiLat has established that anisotropy of irregularity structures in the plane normal to the magnetic field is limited to a narrow belt of geomagnetic latitude associated with the nightside diffuse aurora, ionospheric irregularities elsewhere being elongated only along the field. Understanding this fact in light of the known evolution of convectively developed structures also will be an objective in the Polar BEAR era.

While HiLat has reinforced earlier indications of the overriding importance of convection in irregularity production, it also has introduced a nuance regarding the influence of shears in the convection velocity. Some HiLat and other observations (Basu *et al*, 1986; Bythrow, 1986) suggest a contribution to irregularity development by shear-driven instabilities in addition to those already known to develop in a uniform convective flow. An objective during Polar BEAR will be to establish whether shear is a significant factor in development of scintillation-producing irregularities or only a minor influence in determining irregularity configuration.

The Polar BEAR satellite itself will contribute in several ways to meeting the objectves of DNA's high-latitude HANE program and the closely related objectives of AFGL's program of ionospheric research. First and foremost, its visual/ultraviolet imager will provide macro-scale plan-view images of the aurora, both at

night and in broad daylight, to provide a context in which to relate data from the other HiLat and Polar BEAR sensors to global-scale ionospheric/magnetospheric processes. This objective was not met by HiLat due to early-mission failure of its imager. The effort will be augmented by the improved magnetometer on Polar BEAR, which will be used not only for determining spacecraft attitude and therefore image registration, but also to relate the auroras imaged and other phenomena detected by HiLat and Polar BEAR to major systems of field-aligned currents flowing between the ionosphere and the magnetosphere.

A second specific objective of Polar BEAR is to extend observations of radiowave scintillation into the rising phase of the new solar-activity cycle, even if the now-three-year-old radio beacon on HiLat should fail. While both are operating, an objective will be to obtain double or multiple looks (using both satellites and two or more ground stations simultaneously) through the ionosphere to sort out questions of aspect sensitivity, spatial variation, and temporal development in scintillation-producing structures, using Polar BEAR's images as a guide to interpretations.

SECTION 3

HILAT

3.1 OPERATIONAL HISTORY.

The HiLat Satellite was launched on 27 June 1983, carrying five experiments. Table 1 lists the experiments, their intended purposes and basic characteristics, and the principal experimenters associated with each. Data are collected by means of real-time transmissions to the four high-latitude receiving stations shown by encircled stars in Figure 1, which are as follows: Tromso, Norway (auroral zone); Sondre Stromfjord, Greenland (polar cusp); Churchill, Manitoba (auroral zone); and Bellevue, WA (plasmapause). A fifth station (non-circled star) operates sporadically at Inuvik, Northwest Territories (auroral cusp). The Bellevue receiver, nicknamed Rover, is transportable to other locations for limited-duration observing campaigns.

The experiment payloads normally are operated over the northern quadrisphere of the earth, although they can be turned on for any quarter of the orbit. The satellite is in an approximately 800-km circular orbit at 82° inclination, and the orbital plane precesses through 24 hours of solar time approximately twice per year.

Following launch, all HiLat experiments operated as designed, with the exception of the electron sensor (Langmuir probe) of the plasma monitor. The connection from its electronics package to the outer grid of the probe was severed during launch or orbital insertion, resulting in a locally floating ground. The probe continues to detect electrons, but they are of unknown superthermal energy rather than the ambient thermal electrons for which the sensor was designed.

More distressingly, the high-voltage power supply to the imaging vacuum-ultraviolet spectrophotometer in the AIM (Auroral Ionospheric Mapper) optics package failed after producing several tantalizing images of both the nightside and dayside aurora. Images were produced simultaneously with collection of energetic-electron spectra and data from the magnetometer and plasma probe on approximately forty passes during the engineering initialization phase of the mission. Unfortunately the failure occurred prior to activation of the fully equipped HiLat receiving stations for the operational phase of the mission. Consequently, beacon data were not collected simultaneously with production of images, which therefore now constitutes a major goal of Polar BEAR.

Table 1. The HILAT experiments.

Leon Wittwer (DNA), Program Manager

PAYLOAD	OBSERVABLES	CHARACTERISTICS	EXPERIMENTERS
BEACON	Scintillation Total Electron Content (TEC)	138, 390, 413, 436 MHz 1239-MHz reference Circular polarization	Carlson et al (AFGL) Forsyth et al (UWO) ¶Fremouw et al (PDNW) *Rino et al (SRI)
PLASMA MONITOR	$\Delta(\text{Log } N_e)$, N_e, T_e N_i, N_{O+}, N_{H+}, T_{H+} $\vec{V}_d \Rightarrow \vec{E}$	Langmuir Probe[1] Retarding-potential Analyzer (RPA) Resolution to 5 km Ion Drift Meter (IDM) Resolution to 400 m	Hanson (UTD) Heelis (UTD) *Rich (AFGL)
ELECTRON SPECTROMETER	Electron Flux & Energies	20 ev - 20 kev Zenith, Nadir, 40° Resolution to 400 m	*Hardy (AFGL)
MAGNETOMETER	$\vec{B}$, $\Delta\vec{B} \Rightarrow \vec{J}$	3-axis Fluxgate[2] Quantization 12 nt Resolution 400 m	Bythrow (APL) *Potemra (APL) Zanetti (APL)
AIM OPTICS PACKAGE	Aurora	VUV Imager[3] 3914 & 6300 Å Photometers[4]	*Huffman (AFGL) Meng (APL)

[1]Failed on launch
[2]Z axis failed 12 June 1985
[3]Failed 23 July 1983
[4]Failed 27 November 1985

DNA = Defense Nuclear Agency
AFGL = Air Force Geophysics Laboratory
UWO = University of Western Ontario
PDNW = Physical Dynamics, Inc., Northwest Division
SRI = SRI International
UTD = University of Texas, Dallas
APL = Applied Physics Lab, The John Hopkins University

¶HiLat Project Scientist
*Experiment P.I.

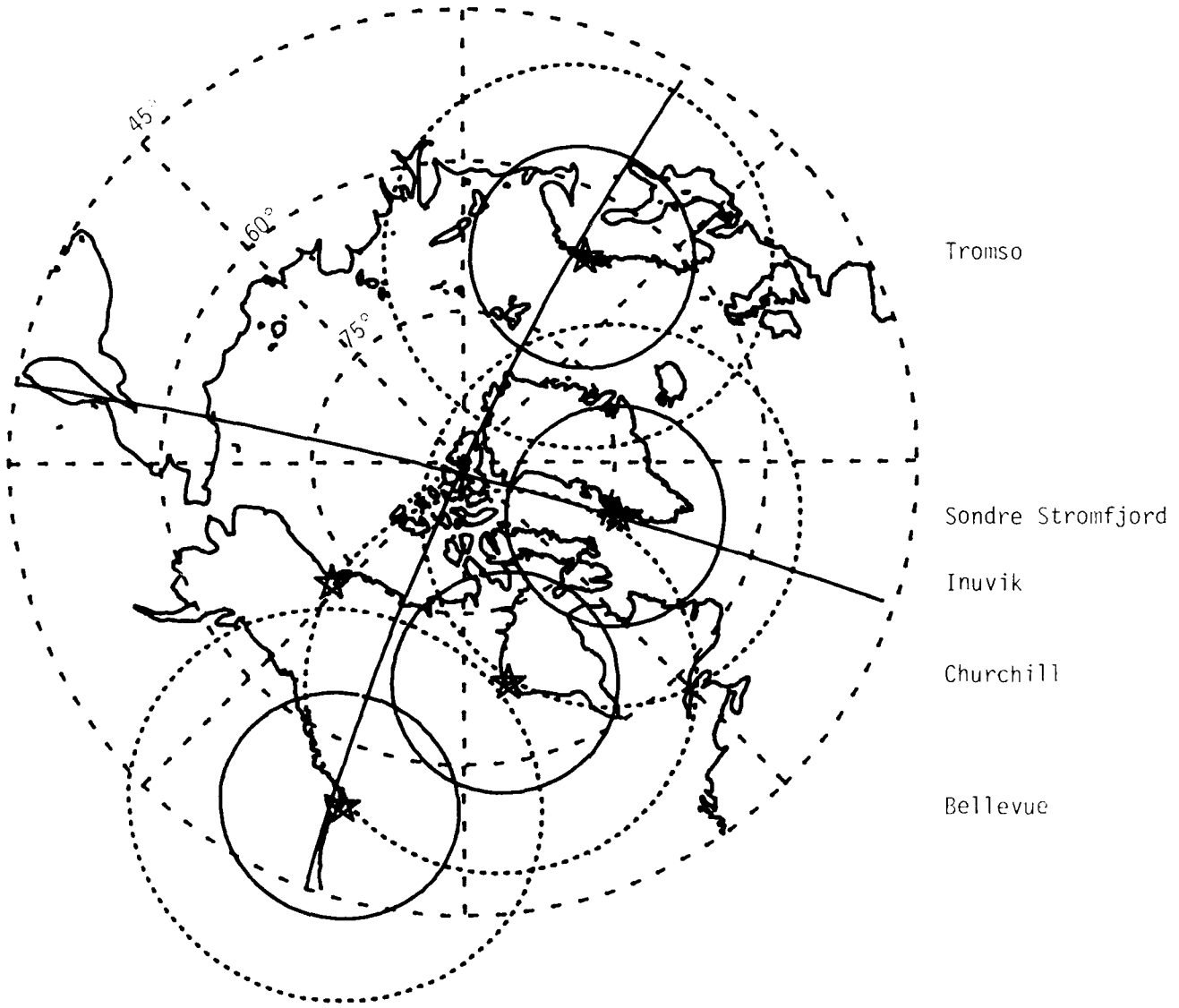

Figure 1. HiLat/Polar BEAR receiving stations and data coverage for HiLat beacon (solid circles) and beacon (dashed) experiments in offset-magnetic-pole coordinates. Two representative passes are shown.

On both HiLat and Polar BEAR, the magnetometer serves a dual purpose. First, it plays a direct scientific role in recording fluctuations in the magnitude and direction of the earth's magnetic field at the satellite height. Especially important in this regard are the x and y sensors, which measure perturbations in the two orthogonal, horizontal components of the field. These components are sensitive to currents flowing in and out of the ionosphere along the highly inclined lines of the main geomagnetic field. The magnetometer's second role is to provide information, along with optical solar sensors, for determining spacecraft attitude. The plasma monitor, electron spectrometer, and optics experiments require knowledge of attitude within a few degrees for data analysis.

Both control and sufficiently accurate determination of attitude have been problems in HiLat. The vehicle is a modified Transit (Oscar) Navy Navigation Satellite, the pitch and roll of which are controlled by a gravity-gradient boom and mass. For HiLat, a momentum wheel was added to control yaw. Attitude was to have been controlled within $\pm 10^\circ$ about all three axes, which has been achieved some of the time. During epochs of full sun, however, these specifications are exceeded. Most notably, yaw oscillations upwards of $\pm 25^\circ$ are experienced when the orbital plane is near the terminator.

Because attitude determination requires identification of the sun's bearing from the satellite, it is directly determinable only on the day side of the earth. Prior to launch, it was planned to extrapolate the attitude determined on the day side by means of dynamic modelling of spacecraft oscillations. After launch, however, unexpected modes of oscillation were noted, and dynamic extrapolation has not been performed. The gravity-gradient boom undergoes sudden bending, due to thermal stresses, as the satellite crosses the terminator. This impulsive bending sets off dynamic oscillations about the pitch and roll axes in an unexpected mode with a period of about ten seconds.

The oscillation is small, on the order of a degree, and is sufficiently evident in the magnetometer outputs that it is not a serious threat to data analysis. The unanticipated dynamic behaviors, however, have precluded routine extrapolation of dayside attitude on the night side of the earth. Instead, nightside attitude is determined only for specific passes of interest, employing plasma-monitor data and an assumption that the ionospheric plasma co-rotates with the earth at middle latitudes. The gravity-gradient boom has been redesigned for Polar BEAR to prevent the complicating dynamic behaviors.

Further difficulty in determining HiLat's attitude has been experienced due to bias changes in the magnetometer. Given knowledge of the three magnetometer biases, three-axis attitude could be determined to within ±2° (±1° with smoothing). The magnetometer biases were carefully measured before launch, but it emerged soon after launch that they were not fixed. The x-axis bias, in particular, drifted at a rate of about 250 nanoteslas (nt) per day early in the mission. The drift approached an asymptote and stabilized at -45,000 nt ± random variations of about 4,000 nt. The y- and z-axis magnetometers showed no steady drift, but their biases varied by about ±1,000 nt. These trends and variations required addition of iterative bias estimation to the attitude-determination code used for routine processing of HiLat data tapes.

After approximately two years of operation, the z-axis magnetometer suffered a sudden shift in bias, which saturated its output and rendered it effectively inoperative. By far the least important of the three magnetometers for scientific use, loss of the z sensor nonetheless did further complicate attitude determination. A means for reasonably accurated determination was devised, however, employing the real-time x and y measurements in conjunction with the International Geomagnetic Reference Field model to estimate z. A totally new three-axis magnetometer will be employed in Polar BEAR.

In November of 1985, the power supply for the AIM photometers failed, terminating all optics measurements from HiLat. The beacon, the ion sensors (RPA and IDM) in the plasma monitor, the energetic-electron spectrometer, and the x-axis and y-axis magnetometers continue to function well and to provide useful data from HiLat.

3.2 A SAMPLING OF RESULTS TO DATE.

Prior to its early demise, AIM produced some spectacular images of the vacuum-ultraviolet aurora, including the first auroral images taken in broad daylight. Some of these images have been published elsewhere (Huffman and Meng, 1984; Schenkel *et al*, 1985; Fremouw *et al*, 1985). Pertinent to the present discussion is that appearing as Plate 1 in the paper by Fremouw *et al* (1985). Figure 2 shows partial data from the *in-situ* instruments recorded during that pass with a makeshift HiLat receiver set up temporarily at the ESRANGE Station at Kiruna, Sweden. At about 69570 sec UT, HiLat passed from the diffuse aurora into the discrete-arc oval on the evening side of the earth (~1940 Magnetic Local Time, MLT)

near 69° magnetic Eccentric Dipole Latitude (ELAT). Dynamic energy spectra from the three directional energetic-electron sensors (Plate 2 in Fremouw *et al*, 1985) showed strengthening and hardening of both precipitating and upwelling electrons as the discrete-arc oval was reached, which persisted until the satellite passed into the polar rain about 100 sec later. After traversing the polar cap, HiLat encountered the morning-side oval near 75° ELAT at about 70000 sec UT.

The two traverses of the discrete-arc oval are demarked clearly in Figure 2 by elevated fluxes of precipitating electrons (JTOT), multiple current sheets inferred from the magnetometer, and directly by the vuv emission recorded in AIM's nadir pixel. The thermal-ion sensors disclosed rapid shear flows in the auroral-oval plasma, with the horizontal ion velocity closely correlated with the magnetic-field perturbations on the evening side. They also showed elevated plasma density on the evening side, including the region of diffuse aurora, as compared with the early-morning side, and some density enhancement associated with the nightside arcs. Although many topside density enhancements are related to precipitating-electron flux, there is by no means a one-to-one correspondence.

The brightest auroral region was one of generally upward current, presumably carried by the precipitating energetic electrons represented in the top trace in Figure 2. The magnetometer, however, indicated an intricate pattern of currents locally flowing downward and upward, as superimposed on an enlarged auroral image in Plate 3 of Fremouw *et al* (1985). The locally strongest current was one flowing downward near HiLat's first encounter with the auroral form. The high-resolution plots in Figure 3 disclose a complex of electrodynamic phenomena associated with the current, as uncovered and analyzed by Bythrow *et al* (1984).

First, direct application of Ampere's law yields an evaluation of the current itself. Specifically, given the orientation of the magnetometer's x, y, and z sensors, the steep inclination of the field lines, and the satellite velocity (7.44 km/sec in the x direction), one finds from the rate of change of the y-component B-field (in nanoteslas/sec) that the field-aligned current was approximately

$$j_z \approx 0.1 \frac{dB_y}{dt} \approx -90 \text{ a/m}^2 , \qquad (1)$$

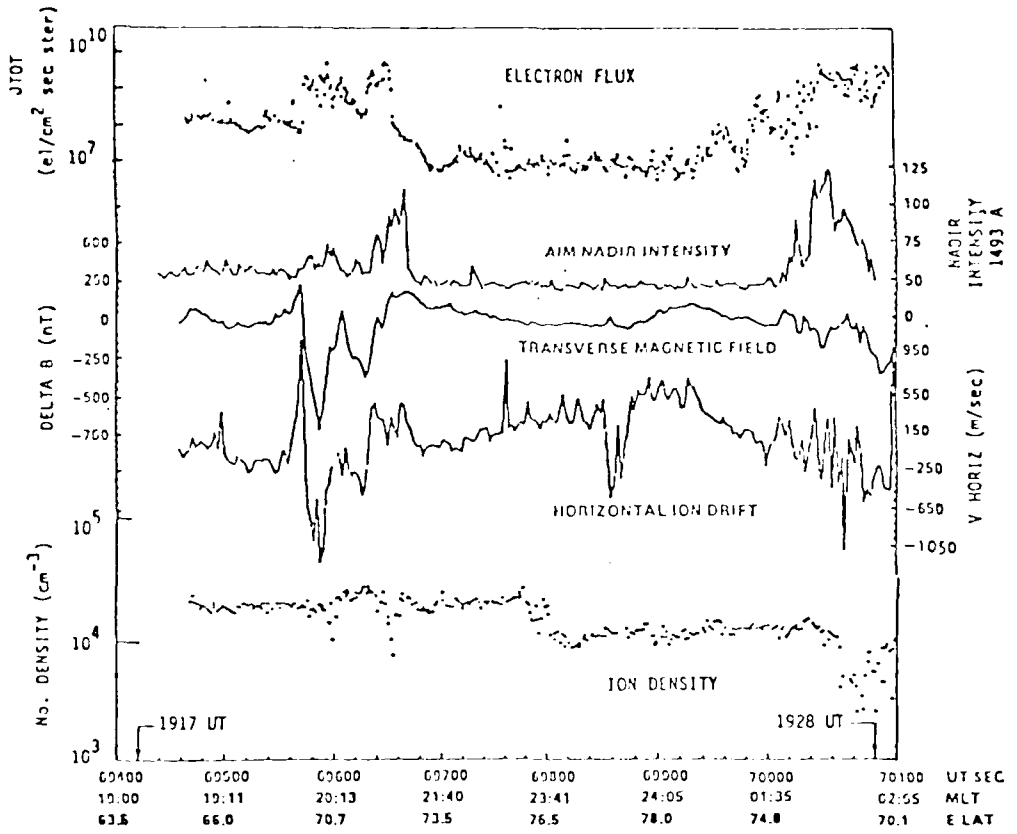

Figure 2. Data from on-board sensors taken during Hilat passage over auroral oval and northern polar cap on 23 July 1983.

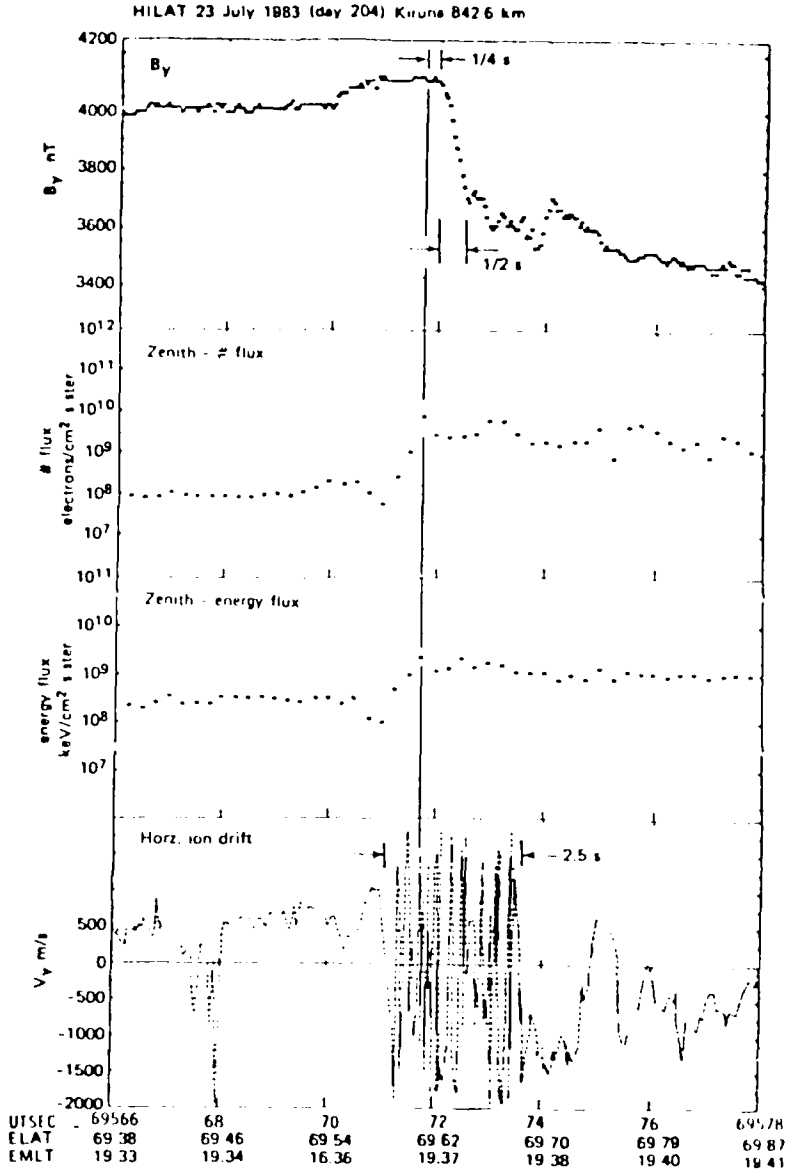

Figure 3. High-resolution data from near the equatorward edge of the [illegible] side auroral oval traversed early in Figure 2. Top: [illegible] magnetometer trace. Middle: number and energy flux of [illegible] electrons. Bottom: cross-track plasma drift measured with ion drift meter. (From Bythrow *et al.*, 1984.)

which is the strongest downward flowing Birkeland current yet observed on any satellite.

The middle two panels disclose a discontinuity in the number flux and energy flux of precipitating electrons about 2 km (1/4 sec) equatorward of the current sheet. Bythrow *et al* (1984) analyzed the electron energy spectra obtained at the foot and at the top of the discontinuity to infer plasma-density profiles and corresponding field-line-integrated Pedersen conductivities. What they found was an x-directed conductivity gradient of 2 mhos/km. Given a minus-x-directed (i.e., southward) electric field of 45 mv/m, the conductivity gradient is sufficient to account for the field-aligned current, as follows:

$$\left(\quad\right)\left(\quad\right) \quad \text{amp/m}^2 \qquad (2)$$

consistent with a value

ity discontinuity,

plasma-velocity variation

gram at Figure 3. These

with the field-

, the current

$$V_e = \frac{J_z}{en_e} \approx \frac{6 \times 10^{10} \text{ el/cm}^2 \text{ sec}}{2 \times 10^4 \text{ el/cm}^3} = 30 \text{ km/sec.} \quad (4)$$

Now, a cross-field gradient length of about 3 km was observed for the precipitating-electron flux from which the Pedersen conductivity was deduced. This combination of plasma-density gradient and drift velocity is ample to trigger the current-convective instability, a member of the family of convective interchange instabilities that plays a dominant role in the development of scintillation-producing irregularities.

Unfortunately, the foregoing observations were made before the complete HiLat stations, with their beacon receivers, were operating. Since that time, however, numerous scintillation observations have been made, ranging from weak intensity and phase fluctuations at the plasmapause (from Bellevue and on a Rover field trip to AFGL at Hanscom Field) to much stronger scintillations observed in the auroral zone and in the polar cap and cusp.

A typical example of polar scintillation and correlative measurements is displayed in terms of reduced parameters on the standard edited-data summary chart reproduced in Figure 4. From top to bottom, the three data panels respectively contain beacon data, parameters relating to auroral precipitation, and information on the density and drift velocity of the thermal plasma at the satellite. Above and between the panels are various scales relating to the location and time of the observations, plus relevant propagation angles. The former include the magnetic apex latitude of the satellite, the F-layer radiowave penetration point, and the F-layer footprint of the field line through the satellite, as well as magnetic (eccentric dipole) time at the satellite.

The auroral-precipitation data include the log of low-energy electron number flux, the vertical current densities derived from the x and y (horizontal) magnetometer sensors, and the log of the output from the nadir-viewing 6300 Å telephotometer (absent in the daytime pass illustrated). The cold-plasma measurements displayed include the ion density from the drift meter and the three component velocities from the drift meter and RPA. (The example shown is from a time prior to automated processing of RPA measurements, so there is no x-velocity trace.)

The panel of beacon data contains measurements of TEC and of intensity and phase scintillation. Specifically, VTEC is the vertical equivalent total electron

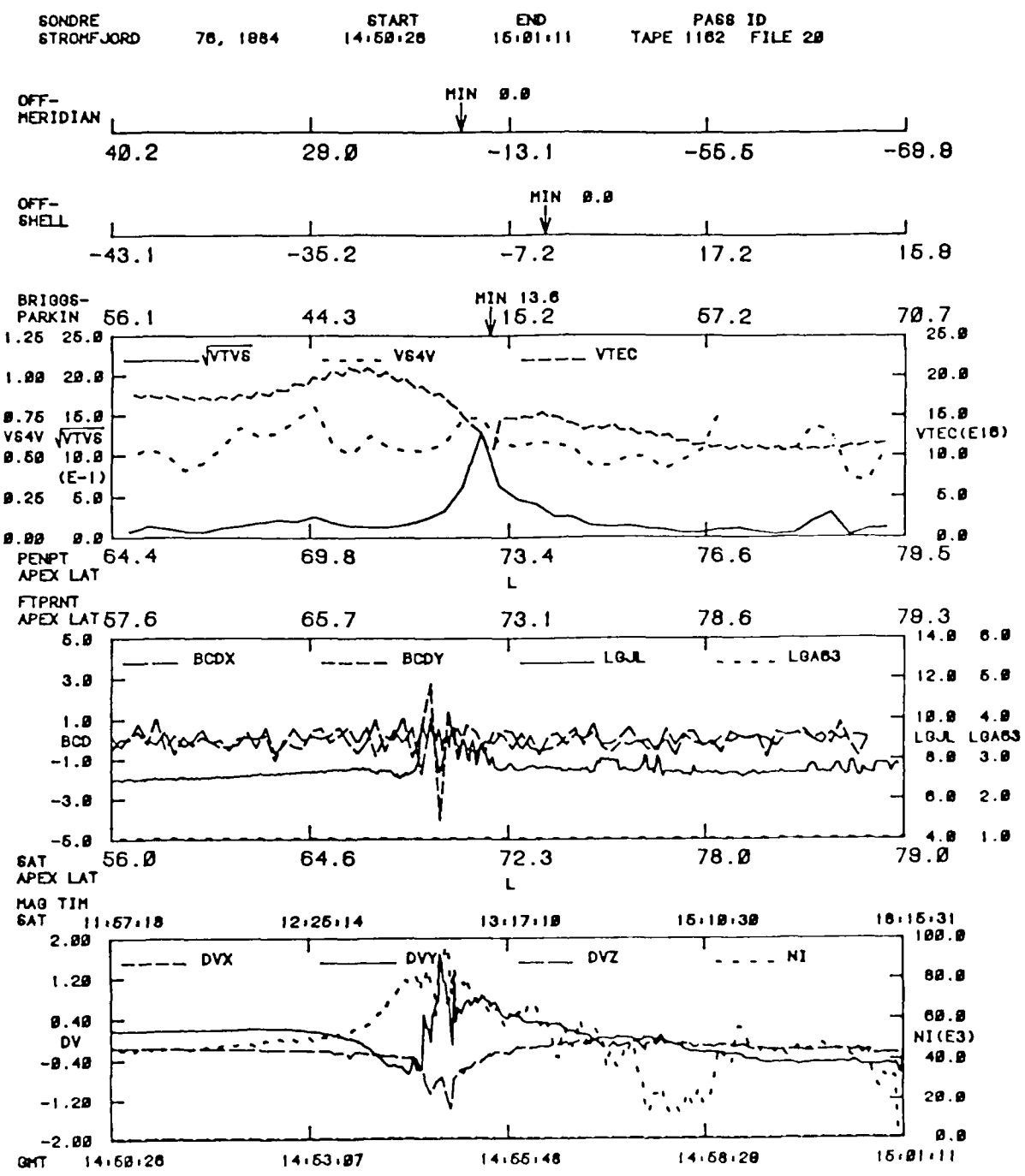

Figure 4. Example of edited and [illegible] amplitude scintillation and TEC data (top panel) and [illegible] parameters obtained from HiLat, recorded at Sondre [illegible] on 1 February 1984.

content, VS4V is the VHF S_4 scintillation index converted to an equivalent vertical measurement, and the remaining (solid) curve is a phase-scintillation index. Both the intensity and phase scintillation indices are edited automatically according to criteria chosen to exclude dead channels, interference, and the like.

For phase, the VHF index is scaled from UHF if the former is contaminated and the latter passes all editing tests. The S in VTVS stands for "scaled" to indicate this possibility. The basic parameter, T, is the power spectral density (PSD) at a fluctuation frequency of 1 Hz (Rino, 1979) derived from a single-regime power-law fit through the fast Fourier transform of the phase time series measured over a 30-sec window. This PSD is divided by the secant of the radiowave incidence angle on the F layer to produce an equivalent vertical parameter. Finally, the square root of VTVS is taken to produce a parameter proportional to the electron-density fluctuation rather than its square.

The dominant scintillation feature of the pass shown, which occurs on many passes, is the four-fold increase in $\sqrt{VTVS}$ near the point of closest alignment of the radio propagation vector with the magnetic field line at the F-layer penetration point (indicated by the minimum in "Briggs-Parkin" angle). While T has been converted to a vertical equivalent parameter, VTVS, otherwise it has been left unadjusted for geometrical effects. The proximity of the prominent scintillation feature to the magnetic zenith, therefore, is an indication that it resulted from geometrical enhancement by anisotropic irregularities.

Moreover, the fact that the feature occurred at the minimum off-field (Briggs-Parkin) angle and not as the line of sight grazed through the local L-shell (minimum off-shell angle = 0) indicates that the anisotropy was field aligned, in contrast to the additional cross-field anisotropy experienced in the night-side auroral oval at latitudes such as that of Poker Flat (Fremouw *et al*, 1977; Rino *et al*, 1978). It is interesting to note, also, that the most prominent TEC feature observed on this pass was an apparent "hole" also co-located with the point of closest approach to the magnetic zenith. Thus, field alignment of large-scale structures (transverse wavelengths greater than 60 km, say) can reveal itself in TEC readings.

The overall effect on phase scintillation of field-aligned anisotropy in irregularity structures is illustrated in Figure 5, which has been obtained from an [illegible] plots like that of $\sqrt{VTVS}$ in Figure 4, displayed on a grid of (the [illegible] angle between the line of sight and (x) the magnetic meridian plane

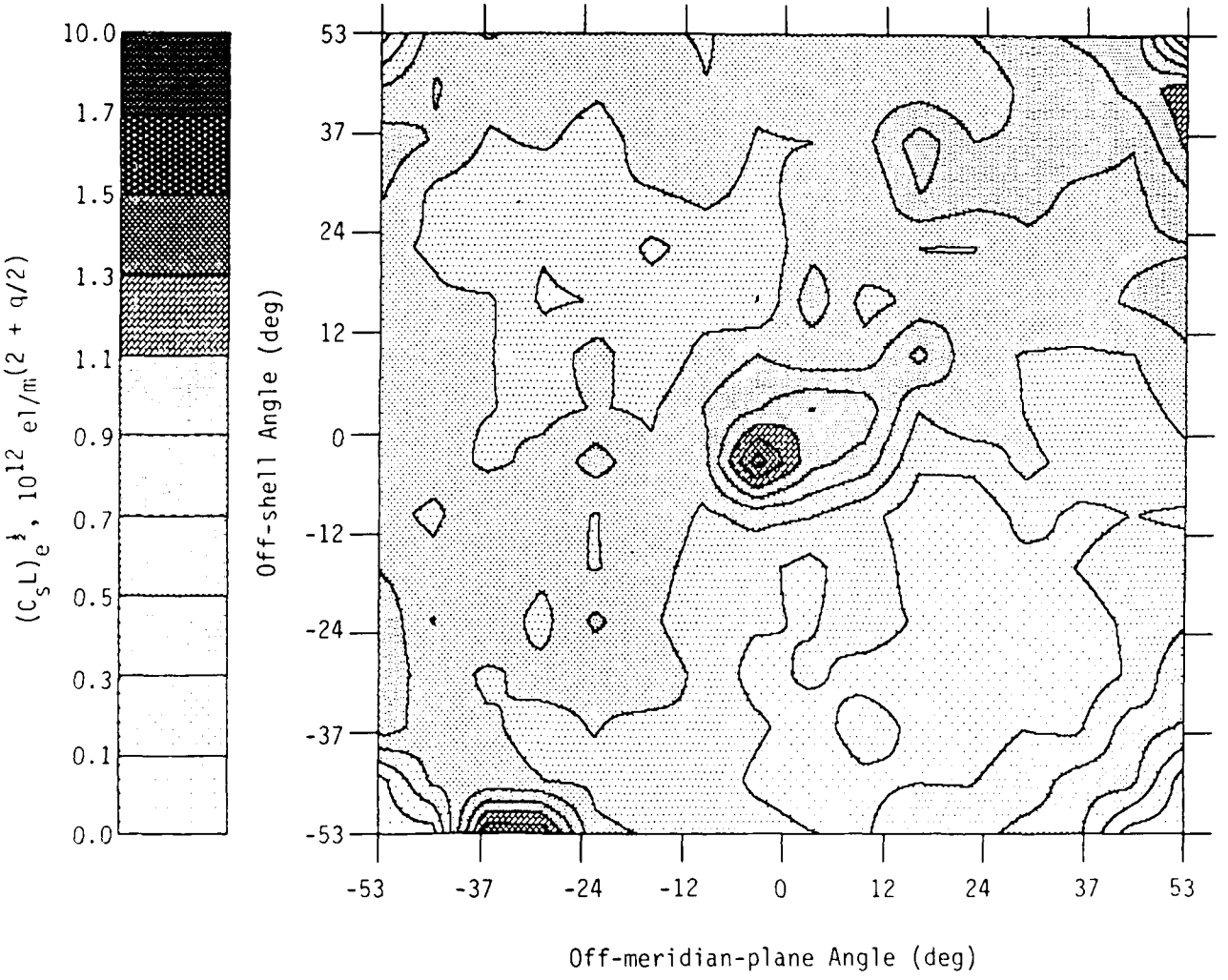

Figure 5. Contours of the geometrically enhanced equivalent height-integrated strength of irregularities causing phase scintillation in the HiLat data base from Sondre Stromfjord between Day 249 of 1983 and Day 123 of 1985. The grid represents (the sine of) the angles between the line of sight and (x) the magnetic meridian plane and (y) the magnetic L shell, both computed at an F-layer height of 350 km. The enhancement near the magnetic zenith (center of the plot) is the signature of axially symmetric irregularities (striations) aligned along the magnetic field.

and (y) the magnetic L shell. The quantity plotted is the spatial-spectral counterpart of the observed temporal PSD (in units that depend upon a power-law spectral index, q), converted from $\sqrt{VTVS}$ by means of the line-of-sight scan velocity through the F layer. It is the equivalent height-integrated spectral strength of the irregularities -- that is, their true strength geometrically enhanced by propagation effects near the point where the line of sight grazes the long axis of the field-aligned structures.

Figure 5 contains all data obtained at the polar HiLat station, Sondre Stromfjord, during about the first twenty months of its operation. The behavior it shows is quite different from that observed in the auroral zone by means of the Wideband Satellite. Those observations, made at Poker Flat, Alaska, showed geometrical enhancement stretched along the x axis of a similar plot, which is the signature of sheetlike (as opposed to axially symmetric) irregularities aligned along L shells. The strongest consistent signature of anisotropy so far observed with HiLat is illustrated in Figure 6, which contains the subset of Figure 5 data collected between 17 and 18 hours MLT.

Considerable effort is going into describing and understanding the spatial spectrum of irregularities and the spatial and temporal spectra of the intensity and phase scintillations that they produce. Examples of the phase spectra observed, namely those obtained at VHF and UHF during the thirty-second period that produced the scintillation peak illustrated in Figure 4, are shown in Figure 7. As is generally the case, the two spectra are nearly identical, including the spectral index of 2.8 obtained from their best-fit power laws (the straight lines indicated on the log-log plots).

These are examples of simple single-regime power-law spectra. A large minority of spectra show multi-regime power laws, the nature and origin of which are being pursued by Rino (1985). Whether one works with single-regime fits or fits to the particular regime that Rino refers to as spanning the "intermediate" scales, the aggregate behavior of the spectral index is similar. Figure 8 contains the occurrence histogram of single-regime spectral indices obtained from all observations made at Sondre Stromfjord during 1984; it peaks sharply near 2.7. Moreover, a portion of its spread stems from a small but interesting trend in spectral index as a function of the off-magnetic-field (Briggs-Parkin) angle of the line of sight, as illustrated in Figure 9.

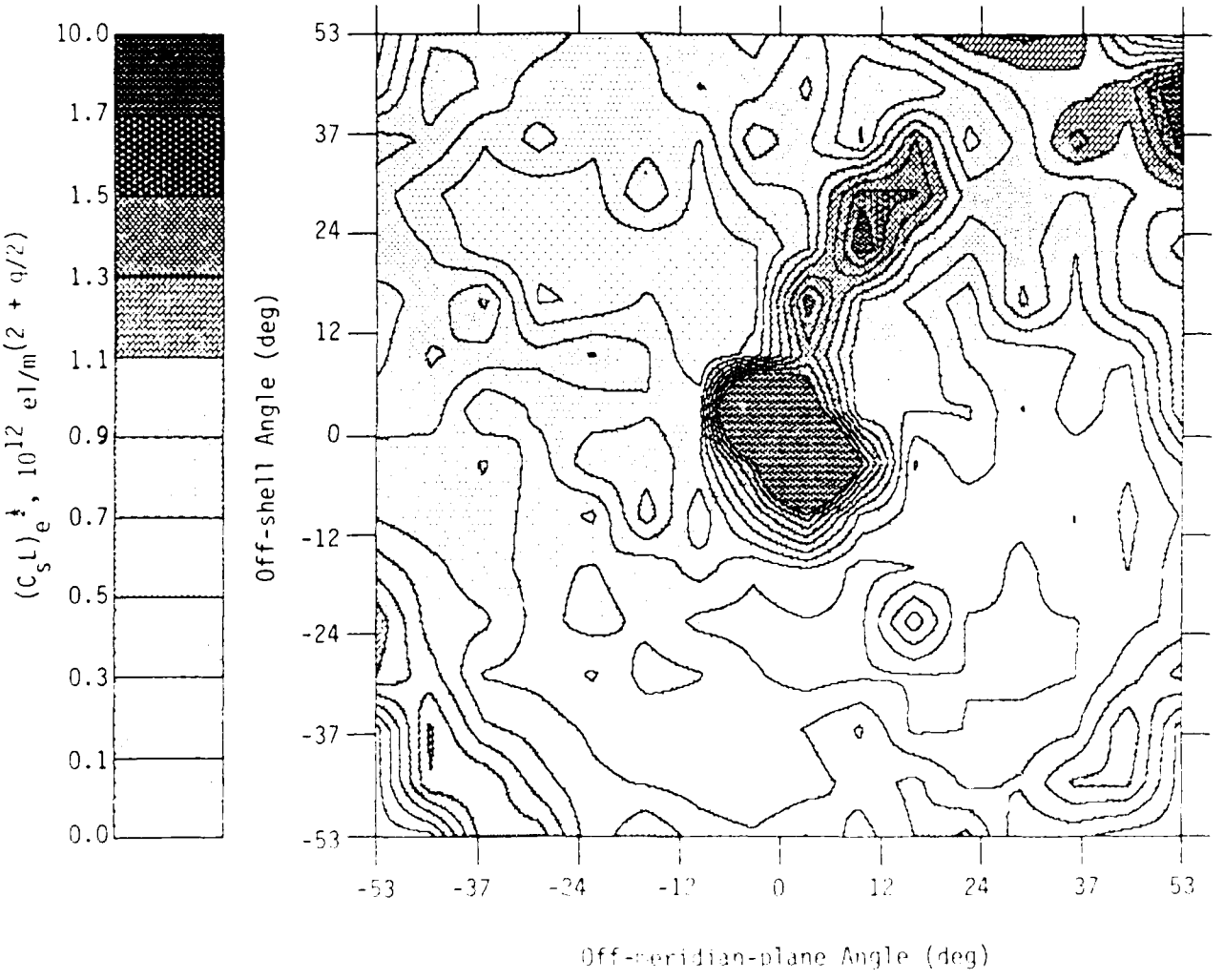

Figure 6. The two-hour sector around 12 hours magnetic local time, which displays the strongest structure of field-aligned anisotropy.

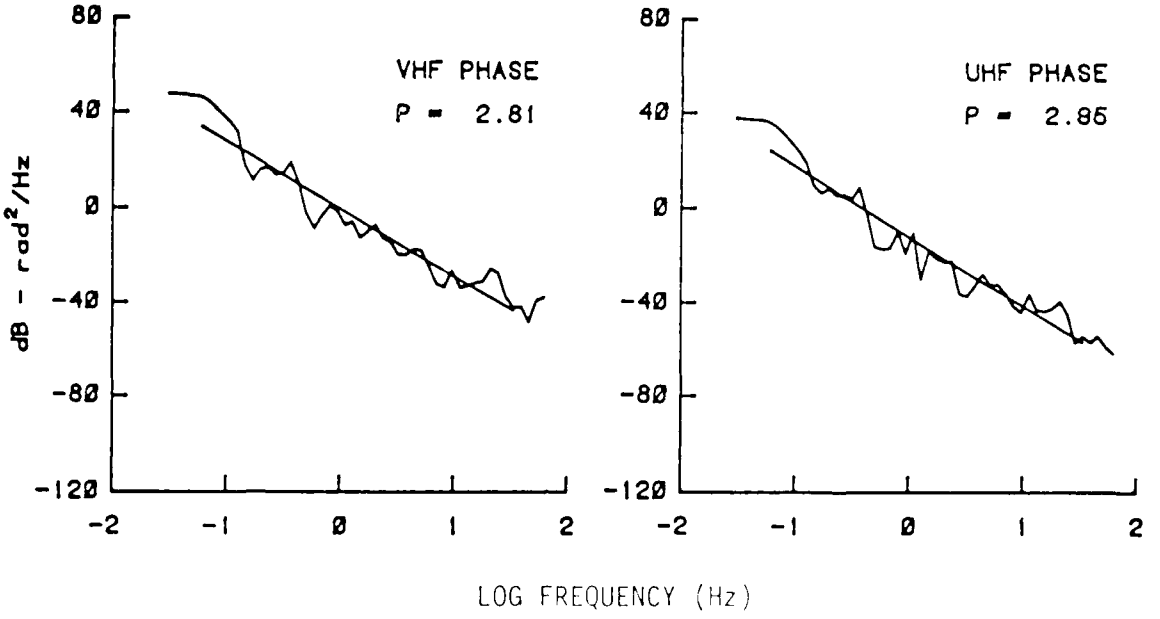

Figure 7. Power spectra of VHF and UHF phase scintillation recorded during the scintillation peak illustrated in Figure 4. The power-law spectral index obtained from the linear fits indicated in these log-log plots is designated p.

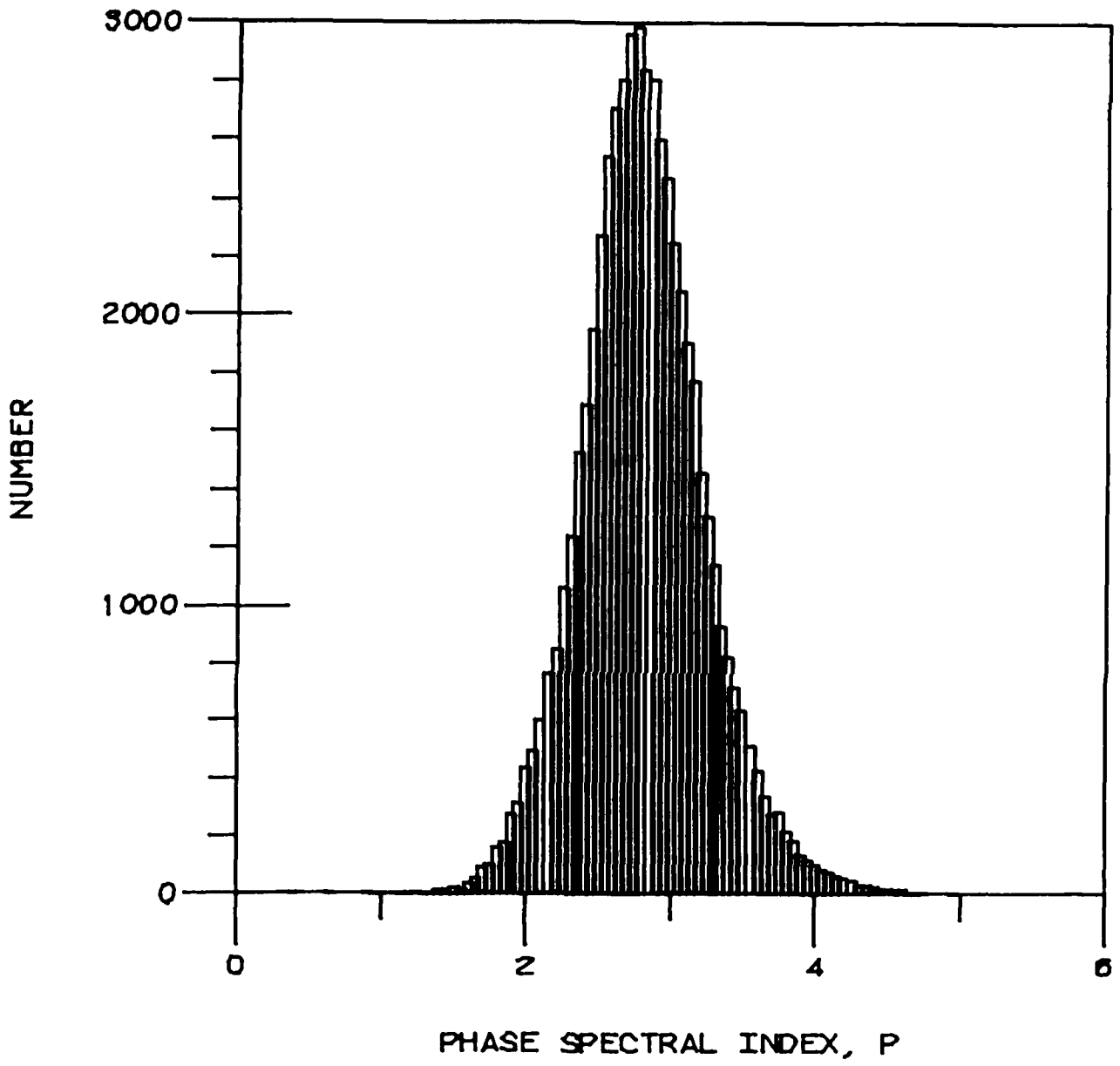

Figure 8. Occurrence histogram of the power-law index obtained from single-regime best fits to phase spectra observed at Sondre Stromfjord during 1994.

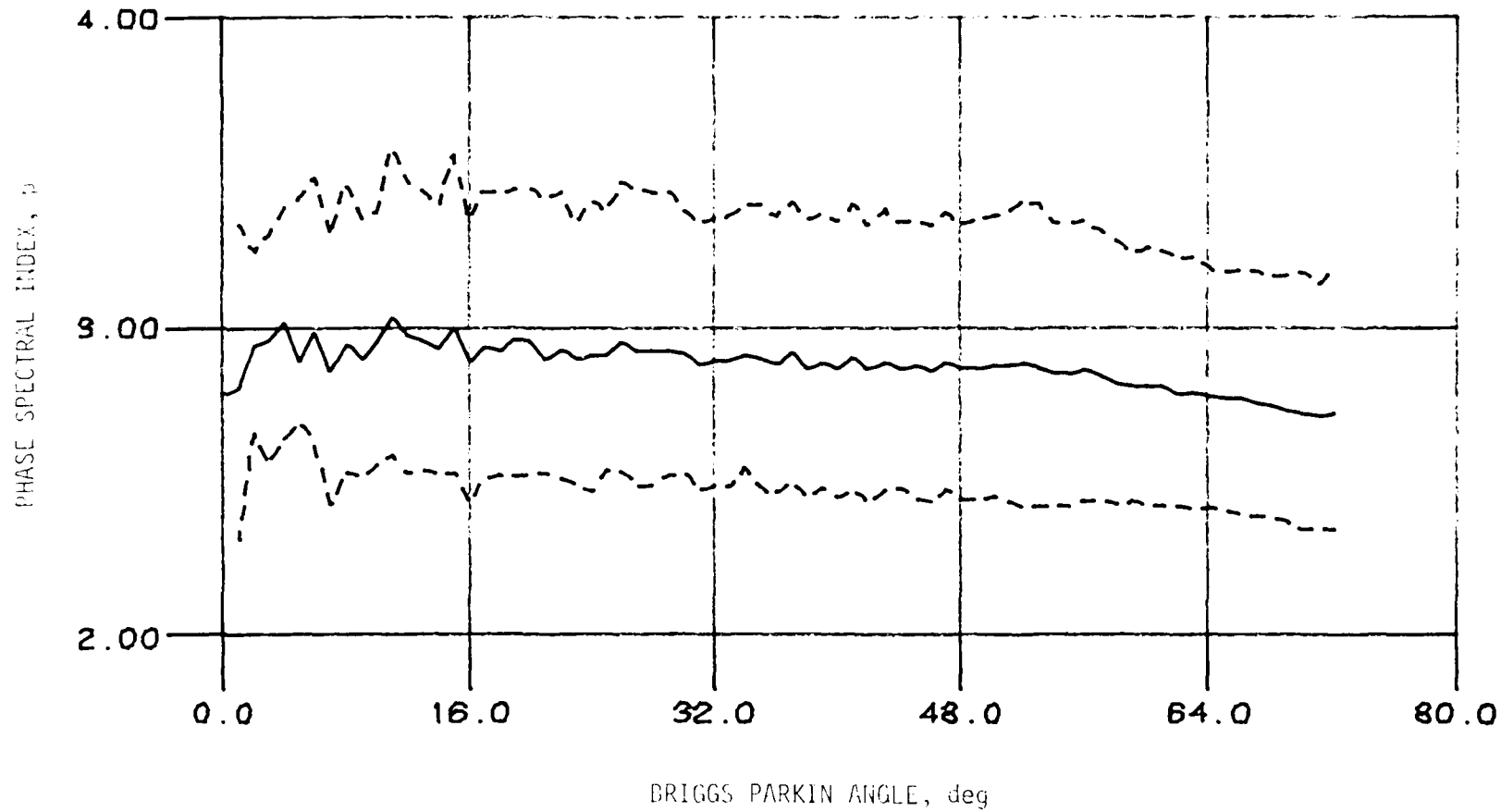

Figure 9. *The mean and standard deviations of phase spectral index, p, for the data population contained in Figure 4, as functions of the angle between the radio line of sight and the magnetic zenith.*

SECTION 4

THE POLAR BEAR EXPERIMENTS

To meet the specific objectives outlined at the end of Section 2, a combination of three experiment packages will be flown on the Polar BEAR satellite. By means of these payloads, it will be possible to (1) observe complex-signal scintillations at VHF and UHF and infer ionospheric TEC from measurements of radio-frequency dispersion; (2) measure the three-dimensional vector magnetic field at 1000 km altitude and infer the presence and strength of field-aligned and other electric currents; and (3) make plan-view extrapolations and interpolations of measurements being made with Polar BEAR and HiLat, by means of visual-wavelength and ultraviolet (uv) images of both the nightside and dayside aurora (the latter at vacuum ultraviolet, vuv, wavelengths).

The main features of the Polar Bear instruments are summarized in Table 2, along with their P.I.'s and collaborating investigators from participating organizations. The following instrument sketches have been assembled from information provided by the organizations with which the three P.I.'s are affiliated.

4.1 BEACON.

The aspect-sensitivity and spectral behaviors of scintillation discussed in conjunction with Figures 4 through 9 show a good deal of consistency with the corresponding behaviors observed with Wideband, and yet they present interesting and pertinent departures from them. The general power-law nature of the spectra, including the existence of multiple regimes, is quite consistent in results from the two experiments, not only at high but also at low latitudes (the latter explored by Wideband). So also is the fact that the observed phase spectral index is somewhat smaller than three, which was the value expected *a priori*.

A possibly pertinent difference between Wideband and HiLat is that the most frequent spectral index observed in the former was still smaller (2.5) than that observed in the latter (2.7). One overall difference between the two missions is that Wideband was carried out during the rising phase of the solar activity cycle, with a year's worth of data being collected during which the sunspot number was between about 60 and about 120, whereas HiLat was launched during the waning phase of the cycle, with nearly all data so far being collected at sunspot numbers below 60.

Table 2. The POLAR BEAR experiments.

Leon Wittwer (DNA), Program Manager

PAYLOAD	OBSERVABLES	CHARACTERISTICS	EXPERIMENTERS
BEACON	Scintillation Total Electron Content (TEC)	138, 390, 413, 436 MHz 1239-MHz reference Circular polarization	Carlson et al (AFGL) Forsyth et al (UWO) ¶Fremouw et al (PDNW) *Rino et al (SRI)
MAGNETOMETER	$\vec{B}$, $\Delta\vec{B} \Rightarrow \vec{J}$	3-axis Fluxgate Quantization 12 nt Resolution 400 m	Bythrow (APL) *Potemra (APL) Zanetti (APL)
AURORAL/ IONOSPHERIC REMOTE SENSOR (AIRS)	Aurora Airglow	Visual/UV Imager 6300‡ & 3914 Å or 2250 & 3371 Å VUV Imager 1100 to 1800 Å Two lines, $\Delta\lambda$=240 Å VUV Spectrophotometer 1100 to 1800 Å	Del Greco (AFGL) *Huffman (AFGL) Meng (APL)

‡Could be 5577 Å instead (See Section 4.3)

¶Polar Bear Project Scientist

*Experiment P.I.

A relevant question is whether the difference in phase spectral index reported in the two missions is related to solar-cycle epoch or some other truly geophysical factor, or is an artifact of slightly different data-processing procedures. This question currently is being pursued; launch of Polar BEAR near solar minimum with an expected lifetime at least equal to (and, hopefully, exceeding) that of Wideband will contribute to answering this question. For this and other reasons, Polar BEAR will carry a beacon similar to that on HiLat.

The Polar BEAR Beacon will transmit coherently on five frequencies: one at VHF, three at UHF, and one at L Band. The frequencies and powers radiated are given in Table 3. As in HiLat, complex-signal scintillation measurements will be made at VHF and UHF, and the triplet of UHF cw signals will be used to obtain TEC from mesurement of the second difference of phase, $\Delta_2\phi$ (Burns and Fremouw, 1970). The L-band signal will serve as a phase reference for the VHF and UHF scintillation measurements, and it will be available for observations of amplitude scintillation at L band.

Table 3. Beacon frequencies and powers.

Band	Frequency (MHz)	ERP* (dBm)	Rcvd. by Isotropic Antenna (dBm)	
			90°el	10°el
VHF	136.676	28.0	-108	-122
UHF	390.082	21.1	-125	-139
	413.028	25.5	-120	-134
	435.974	19.3	-126	-140
L	1239.084	33.8	-121	-135

*Effective Radiated Power

The L-band and VHF transmissions will be with right-hand circular polarization, but the UHF signals will be transmitted with left-hand circular polarization. The difference is to minimize interaction between the UHF and L-band antennas, which are nested volutes mounted on the nadir-facing surface of the three-axis-stabilized spacecraft. The VHF antenna is a tripole mounted on the end of one of the solar panels.

As in HiLat, the L-band signal from Polar BEAR will not be a clean cw carrier. Because the P87-1 spacecraft has no onboard recording capability, HiLat data will be transmitted to beacon and telemetry receiving stations in real time. The L-band beacon channel will carry the telemetered information, at 4098 bps, from the AIRS imager and the magnetometer. A split-phase-modulation waveform will be used to produce a BPSK signal in the L-band channel.

The carrier suppressed in the L-band signal will be reconstituted in resynchronization loops at the ground stations. One difference between the Polar BEAR Beacon and its predecessor on HiLat is that the new instrument will not always suppress the L-band carrier as severely as does the old one. The L-band carrier from HiLat is suppressed by about 30 dB from the level it would have as a cw signal. The suppression in Polar Bear will vary from about ten dB to about 30, depending upon beacon temperature and operating mode.

While Polar BEAR will radiate the same frequencies as HiLat, the method of generating those frequencies will be somewhat different. As shown in Figure 10, the basic oscillator will operate directly at the radiated VHF signal frequency, under crystal control and with temperature compensation. The oscillator output will be divided by four to produce an internal reference frequency of 34.419 MHz. The reference frequency then will be multipled in phase-locked loops to produce the UHF and L-band outputs. All loops will be closed digitally. The end result should be even more stable operation than that enjoyed in HiLat, which could become pertinent in the event of the hoped-for long life of the Polar BEAR mission (i.e., the desire to obtain data near solar maximum).

4.2 MAGNETOMETER.

As did HiLat, Polar BEAR will carry a three-axis fluxgate magnetometer manufactured by Schonstedt Instrument Co. While the inherent capabilities of the two instruments are similar, their designs are quite different. The HiLat instrument is twenty years old, having been developed for attitude determination on the Transit (Oscar) Navy Navigation Satellites, three of which have been refurbished for Wideband, HiLat, and Polar BEAR. As described in Section 3.1, instability in this aging instrument and its magnetic environment on the spacecraft have introduced difficulties in HiLat operation and data analysis.

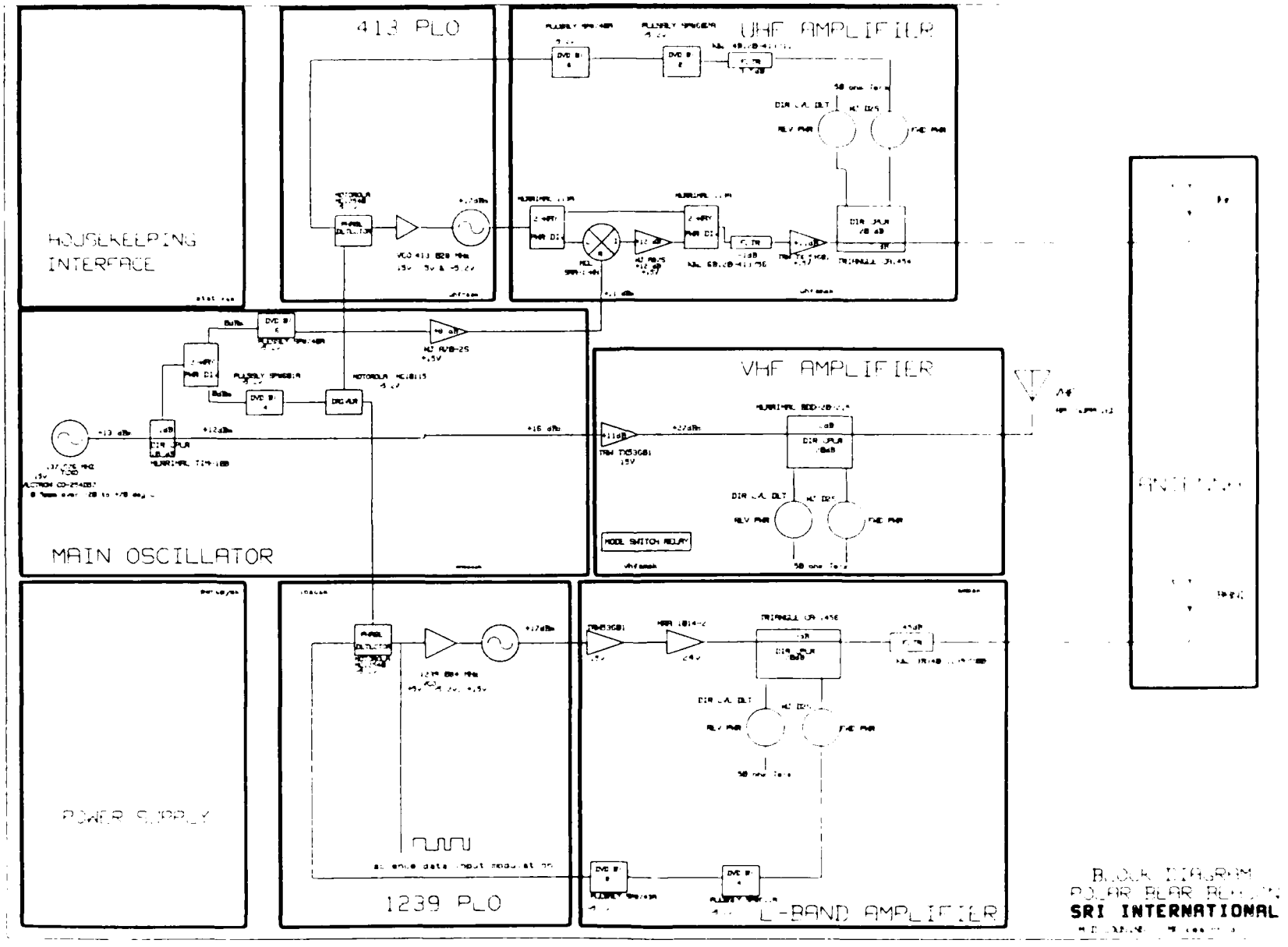

Figure 10. Beacon block diagram. (Supplied by M. Cousins, SRI.)

For Polar BEAR, a totally new magnetometer was specified and acquired. Its design is similar to that used successfully by APL on the Triad Satellite (Zanetti and Potemra, 1982), and its packaging and electronic circuitry are very different from that employed on HiLat. The instrument consists primarily of a three-axis Analog Vector Magnetometer (AVM) and a Magnetometer Data Processor (MDP). The AVM, consisting of the tri-axial sensor unit, an electronics unit, and their interconnecting cables, is depicted in Figure 11. An important feature of the Polar BEAR magnetometer is that the tri-axial sensor unit will be mounted near the end of a solar panel for isolation from magnetic fields generated within the body of the spacecraft.

As in HiLat, the Polar Bear magnetometer will measure a component of the vector magnetic field, with a quantization uncertainty of 12 nt, 60 times per sec. Thus, the vector field will be measured 20 times per sec, yielding a spatial resolution of 370 m. The MDP will sample the three analog outputs of the AVM to 13-bit quantization, compress the data, format it, and transmit the condensed data to the spacecraft's science telemetry system. Data compression is required to achieve the desired spatial resolution within the 384-bps telemetry rate allotted to the magnetometer. Two frames of science data will be transmitted to the ground stations per sec via the L-band beacon channel. The MDP utilizes a small resident microcomputer, designed around the RCA 1802 microprocessor, to perform the foregoing tasks. In addition to the science data, the MDP will provide "telltales" to give an indication of instrument health.

The magnetometer data will be used, hopefully in conjunction with that from HiLat, to map out major current systems flowing between the ionosphere and the magnetosphere, which can contribute to development of plasma-density irregularities via the current-convective instability (Ossakow and Chaturvedi, 1979). In addition, the magnetometer will provide a basis for determining the attitude of the Polar BEAR Satellite. The satellite carries digital solar attitude detectors, sensors for determining the direction to the sun. The measured magnetic-field vector will be used, in conjunction with a model of the earth's field (the International Geomagnetic Reference Field), to resolve the spacecraft rotation angle about the line to the sun. Attitude so determined on the day side of the earth will be interpolated through the night side by means of a model of the spacecraft's dynamic behavior.

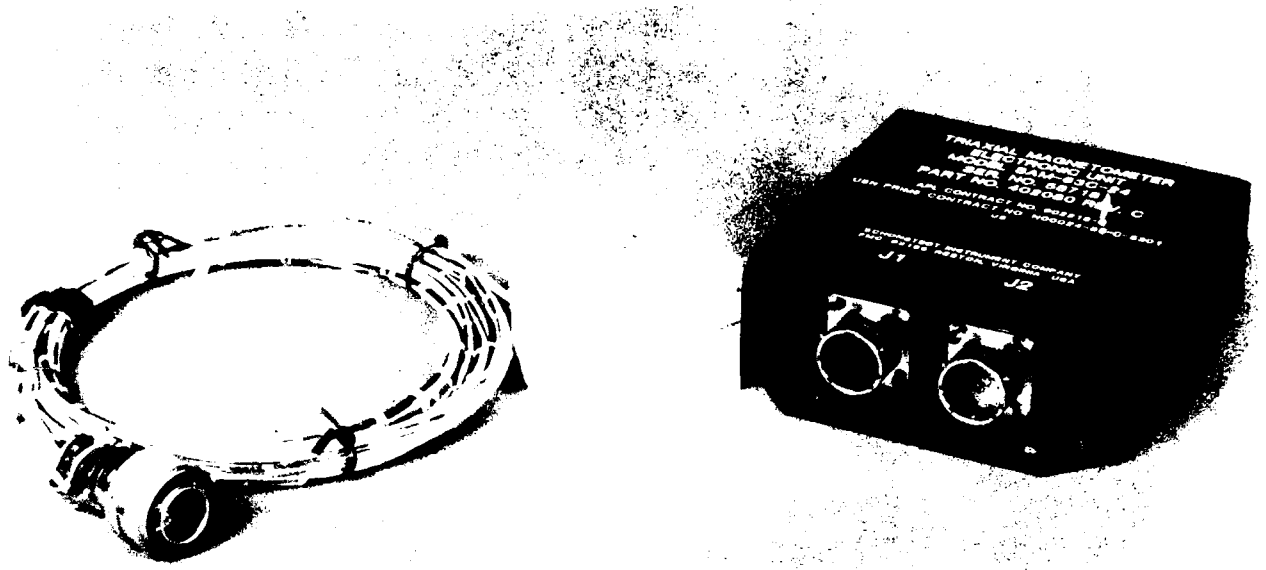

Figure 11. Fluxgate magnetometer. The triaxial sensing unit (center) measures 2.1 x 2.0 x 2.5 in and weighs 0.35 lbs. The electronics unit (right) measures 1.9 x 5.2 x 5.3 in and weighs approximately 1.5 lbs. An associated data processor (not shown) measures 1.9 x 7.0 x 7.6 in and weighs 1.65 lbs. The instrument requires 1.2 watts of power. (Supplied by T. Potemra, APL.)

4.3 AURORAL/IONOSPHERIC REMOTE SENSOR (AIRS).

All the motives for flying the Auroral Ionospheric Mapper (AIM) on HiLat still exist. Foremost among these, scientifically, is the utility of auroral images in providing a phenomenological framework (a macro-scale plan view) within which to relate the myriad interdependent plasma and electrodynamic processes going on in the high-latitude ionosphere. To the scientific motives now have been added direct applications interest in auroral and airglow emissions and their spatial structure as they relate to SDI.

A key feature of AIM, and now its successor, AIRS, is their ability to provide auroral images in broad daylight as well as on the night side of the earth, owing to their operation in the vuv portion of the electromagnetic spectrum. The AIM concept was based on measurements made on the S3-2 Satellite with a fixed vuv spectrophotometer (Huffman *et al*, 1980), which demonstrated the measurability of several vuv spectral lines in the aurora and airglow. Its utility as an imager was demonstrated clearly during its short lifetime on HiLat.

The AIRS instrument, illustrated in Figure 12, will be similar to AIM in the method used to generate images of the aurora, the ionospheric airglow, and their structure, namely a mirror scanning across the satellite track. It will be substantially more informative, however, in that it will be able to produce such images at four wavelengths simultaneously. The imaging capability of AIM was limited to a single (selectable) vuv wavelength. Its only non-vuv capability came from two associated fixed photometers directed at the nadir and operating at 6300 and 3914 Å.

The new instrument will be able to provide simultaneous images at two non-vuv wavelengths plus simultaneous images at any two vuv wavelengths separated by 240 Å in the band between 1700 and 1800 Å. In addition to providing redundancy, the 240 Å fixed separation in the vuv band will permit imaging of emission features from different ionospheric constituent species. An example is the radiative recombination line of oxygen at 1356 Å in conjunction with the 1600 Å line in the Lyman-Birge-Hopfield band of molecular hydrogen. The former may be of particular interest for F-layer studies (Chandra and Reed, 1975).

Alternative to its operation as an imager, the vuv instrument may be operated as a nadir-directed spectrometer by sweeping the wavelength instead of the scan mirror, or it may be operated as a fixed photometer by also stopping the wavelength in its scan. In each mode, the recorded signal will be produced by a pair of

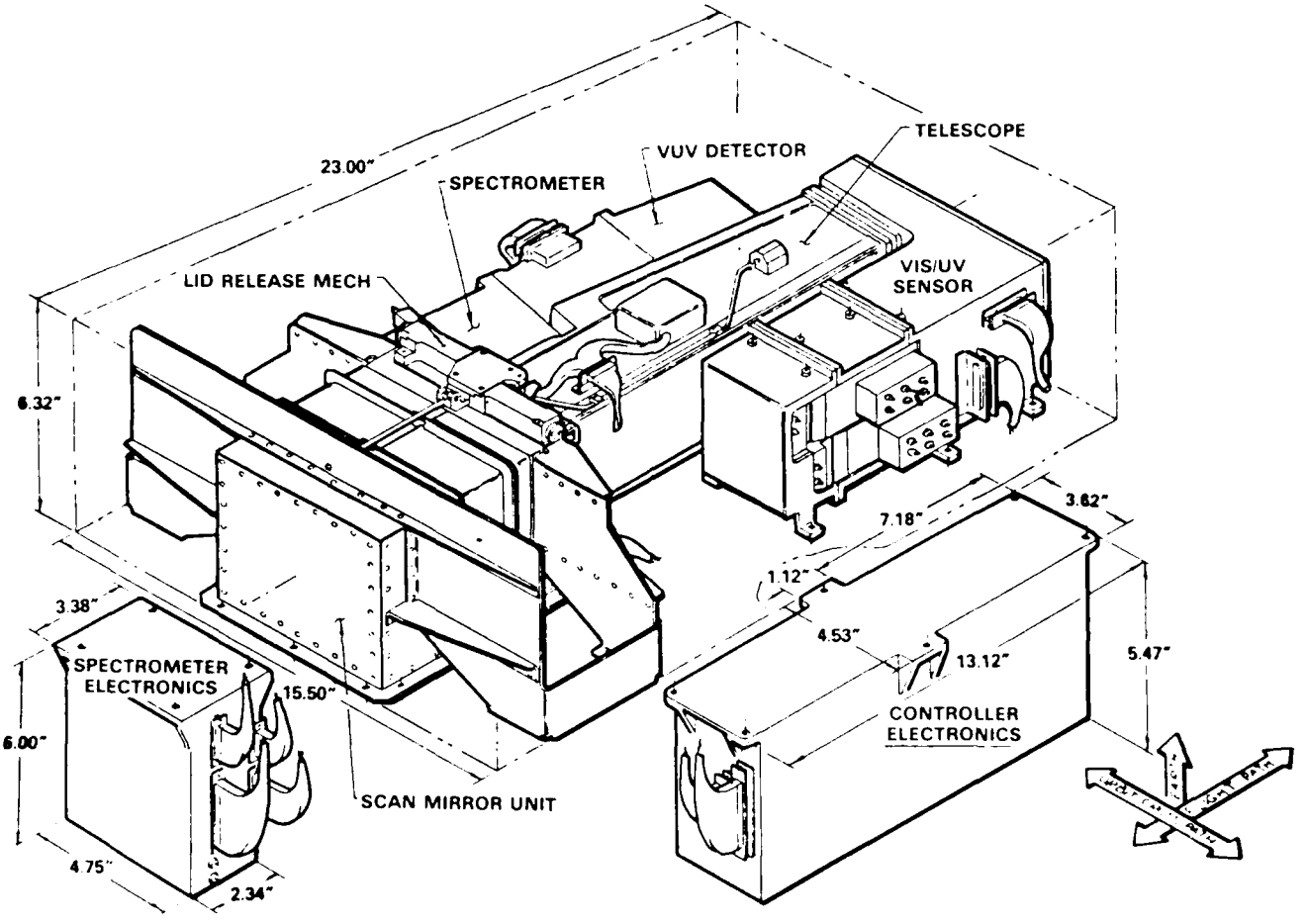

Figure 12. The Auroral/Ionospheric Remote Sensor (AIRS). The main instrument package weighs approximately 22 lbs, and the instrument uses approximately 15 watts of power on average. (Supplied by R. Huffman, AFGL.)

photomultiplier tubes placed at the two exit slits of a modified 125-mm Ebert-Fastie spectrometer. The photomultiplier counts will be converted to Rayleigh intensity units based on instrument calibrations. The threshold of sensitivity to vuv emissions is approximately 50 Rayleighs. The full-width/half-maximum bandwidth is 36 Å.

The non-vuv capabilties of AIRS also are quite varied, in terms of the wavelengths available for imaging by two filtered photometers. At night, images will be developed at 3914 Å (first negative band of ionized nitrogen) in the near uv and either at 6300 Å (radiative recombination of atomic oxygen) in the red or 5577 Å (forbidden transition of atomic oxygen), the auroral green line. The red line is preferred for studies of plasma patches in the polar F layer that are identifiable by means of their bright airglow emission in this line (Buchau *et al*, 1984). Photomultiplier-tube sensitivity is somewhat marginal in the deep red, however, while being totally adequate for the green line, which in any case is brighter. For this reason, it is possible that a final sensitivity check of the particular photomultiplier to be flown may prompt choice of the 5577 Å filter instead of 6300 Å. If so, 1356 Å will receive even more attention as a likely signature of the polar patches.

In the daytime, images will be obtained at 3371 and 2250 Å in the near and middle uv to obtain albedo backgrounds of the atmosphere. At night, these same wavelengths may be used to measure radiation in, respectively, the second positive band of nitrogen and the gamma band of nitric oxide. The non-vuv images will be obtained by passing some of the light collected by the common scan mirror through a small hole in the spectrometer telescope, through the appropriate filters, and on to the photometers.

As did AIM, the AIRS instrument will make line scans of emission intensity in the region below the satellite from slightly above the horizon, through the nadir, to the opposite horizon. The mirror then will return rapidly to the initial position, completing the cycle in three sec. The spatial resolution in the cross-track direction will be approximately five km at auroral altitudes (on the order of 100 km), as set by the count period of approximately seven msec. Along the track, the resolution will be approximately 20 km, corresponding to the three-sec scan period as the satellite moves in its orbit at about seven km/sec.

With fewer ionospheric instruments on Polar BEAR than on HiLat, using the same science telemetry system permits allocation of more information capacity to AIRS

than to AIM in the approximately half-second telemetry frames. The AIRS data rate will be about 3500 bps, and its vantage point at 1000-km altitude will give it larger coverage than was enjoyed by AIM. During a typical high-elevation pass over a given receiving station, it will produce an image covering an area of approximately 6000 km across its track and 5000 km along it (about 45° along a great circle).

SECTION 5

THE P87-1 SATELLITE AND ITS ORBIT

5.1 THE SATELLITE.

The P87-1 spacecraft is a modified OSCAR-class ('O' for Operational) TRANSIT Navy Navigation Satellite from which the navigation electronics have been removed. Following the approach used in P76-5 (Wideband) and P83-1 (HiLat), the OSCAR has been augmented with additional payload-housing structures by APL. Beyond addition of a "pentnouse" as in both Wideband and HiLat and an "experiment deck" as introduced in HiLat, Polar BEAR's separation plane was lowered (as oriented at launch) to retain a cylindrical "pedestal." This combination assembly is approximately four feet long and two feet in diameter. The entire satellite weighs just under 300 lbs.

After orbital insertion, the spacecraft will be turned "upside down," with the pedestal extending away from the earth and the penthouse and experiment deck directed toward the earth. Figure 13 illustrates the spacecraft's operational right-handed coordinate system, with +X directed along the orbital velocity vector and +Z directed toward the earth. As shown in the figure, AIRS and the beacon's UHF/L-band antenna are mounted on the nadir-directed experiment deck, the magnetometer sensor unit on the end of the -X solar panel, and the beacon's VHF antenna on the end of the +X panel.

The four solar panels each measure 66 inches in length and together deliver 35 to 50 watts, averaged over an orbit and depending upon solar illumination angle, to a nickel-cadmium storage battery. In addition to housing the magnetometer sensor unit and the VHF beacon antenna, the solar panels support antennas for receipt of commands and for tracking and transmission of housekeeping (and science backup) telemetry. The latter transmissions will take place at 150 and 400 MHz and will appear as transmissions from the TRANSIT constellation with a frequency offset of -141.6 parts per million.

Three-axis stabilization will be provided to within $\pm 10^{\circ}$ by a 60-foot gravity-gradient boom extending toward the zenith and a momentum wheel mounted on the side of the pedestal. Gravity-gradient control of pitch and roll is standard for the OSCARs, a momentum wheel having been added to HiLat and Polar BEAR for control of yaw. The boom orientation is opposite to that normal on OSCARs, on which it

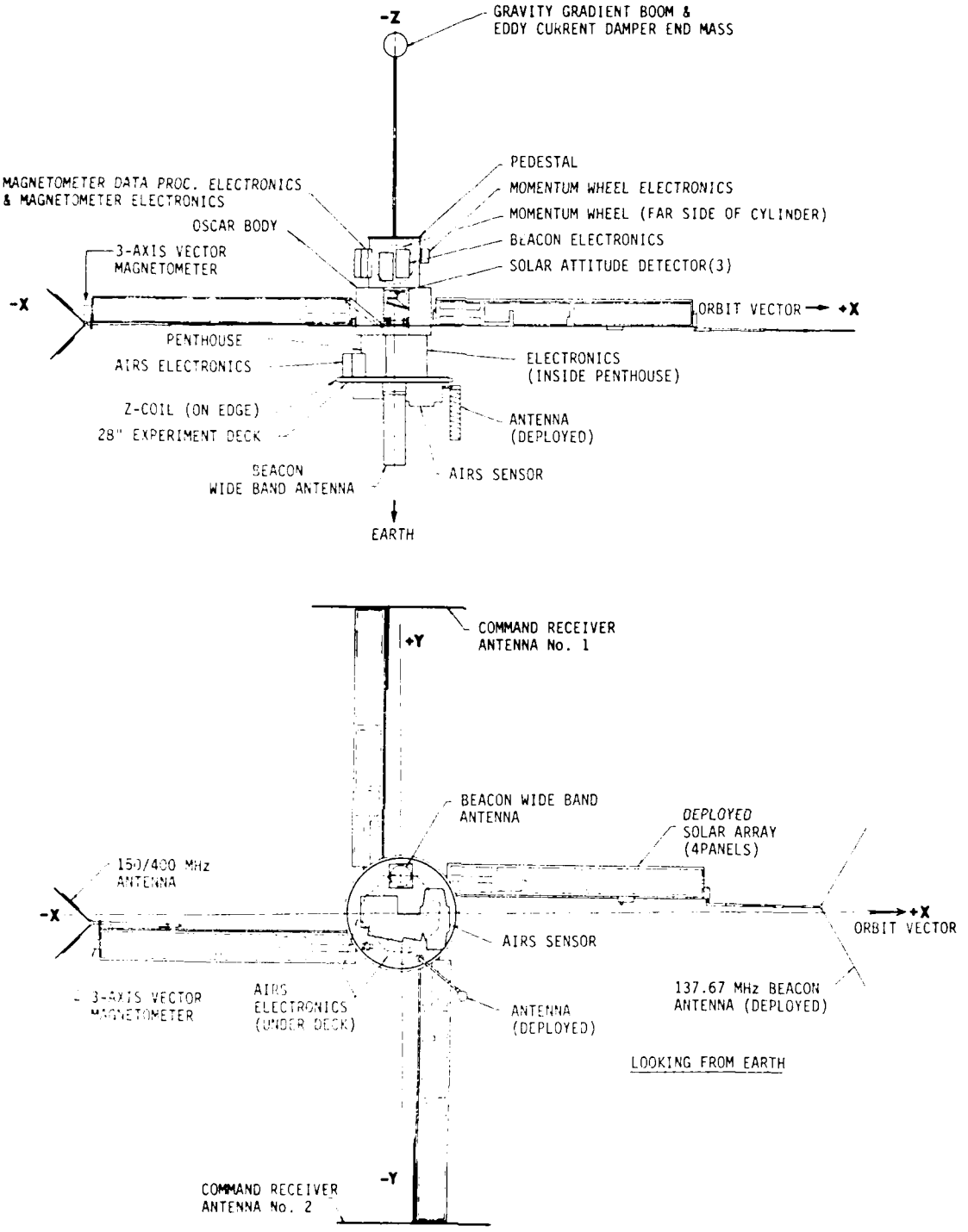

Figure 13. Two views of the Polar BEAR Satellite. Top, looking from its "right side." Bottom, looking from the earth. The spacecraft's right-handed coordinate system is such that +X is directed along the nominal orbital velocity vector, and +Z is directed toward the earth. (Supplied by L. Grant, APL.)

usually "hangs" toward the earth. It was moved to the opposite end of the spacecraft for Wideband, HiLat, and Polar BEAR to make room for an unobstructed earth view by the nadir-directed experiments. Attitude will be measured to within 2° by means of optical sun sensors and the magnetometer and then telemetered to the ground in the science data stream.

A full description of P87-1 is given in the Polar BEAR Mission Interface Control Document, prepared by APL as Document JHU/APL SDO/PAO-0817, dated August 1985.

5.2 THE ORBIT.

Relieved of HiLat's responsibility to perform *in-situ* measurements of plasma density, temperature, and velocity, Polar BEAR will be placed in a higher orbit, still better suited to beacon measurements through the ionosphere and broad-view remote sensing (imaging) of it. It will be in an almost circular orbit near 1000 km altitude, similar to that used very successfully for beacon measurements from Wideband. Specifically, its apogee and perigee will be 1070 km and 930 km, respectively, yielding an eccentricity of 0.01 and an orbital period of 105.1 min.

With its orbital velocity near 7.3 km/sec, high-elevation passes over a station will take just under 18 min from horizon to horizon and just over 14 min above 10° elevation. Figure 14 is a plot of maximum elevation achievable at a high-latitude receiving station, Sondre Stromfjord, Greenland, during a representative 24-hour period, in this case the day that the orbital plane is overhead there at about 12 and 21 hours. Passes reaching a maximum elevation of at least 30° can occur in two periods (containing respectively ascending and descending passes) of approximately 4½ hours duration centered on the overhead times, which change as the orbit precesses. Similar plots may be made for any station, becoming more symmetrical and the minima deeper as the station moves to lower latitudes.

Unlike Wideband, which was in a sun-synchronous orbit, Polar BEAR's inclination has been chosen, as was HiLat's, to produce fairly rapid precession in local time. Its inclination, in fact, will be the same as HiLat's, 82°. Given Polar BEAR's altitude near 1000 km, this will produce a precession rate such that the orbital plane and station maximum-elevation curves, such as that in Figure 14, will move 7 min 17 sec earlier (in solar time) each day. Thus, by observing both ascending and descending passes, a station may obtain measurements at all local times in just over a calendar quarter.

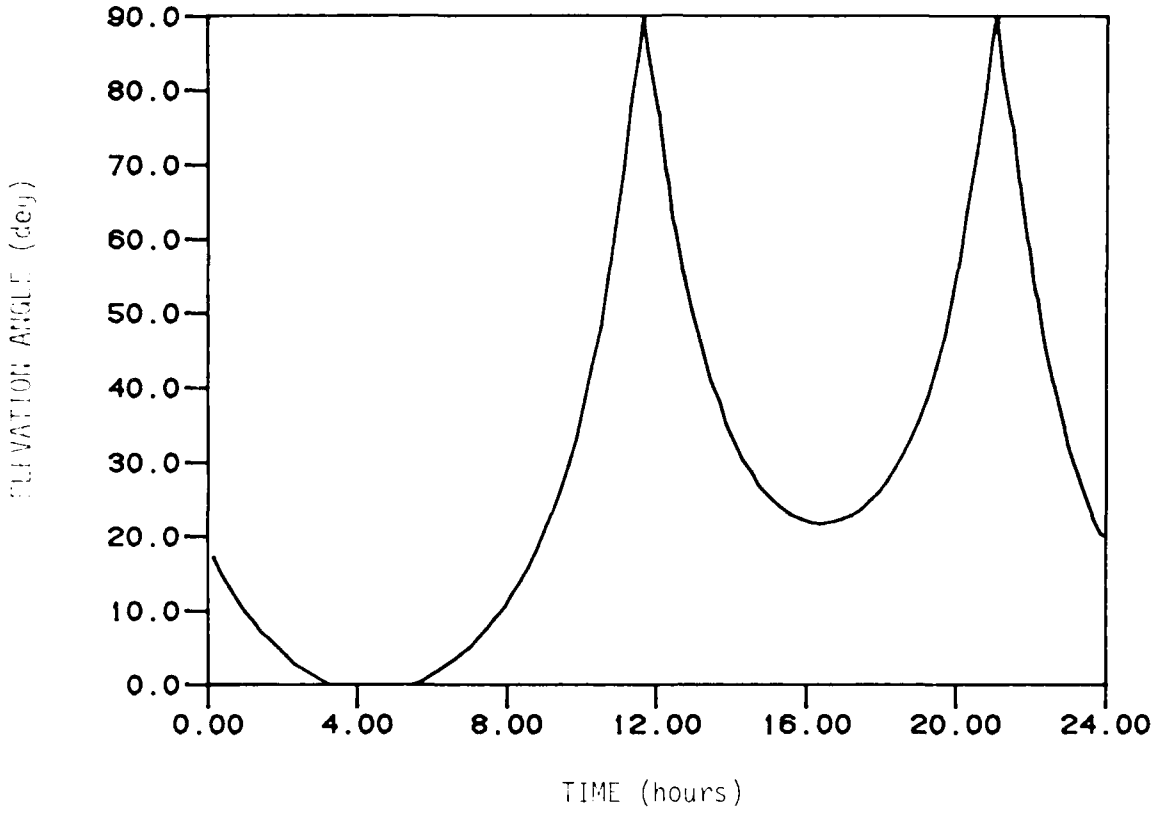

Figure 14. Maximum elevation angle achievable by Polar BEAR in its nominal orbit during passes over a high-latitude station, Sondre Stromfjord, Greenland, in a representative 24-hour period.

Figure 15 illustrates the effect of precession on observations at a station such as Sondre Stromfjord during a representative calendar quarter. The bands of short vertical dashes depict portions above 10° elevation of passes whose maximum elevation is at least 30°, thus falling within the two peaks of Figure 14 (which corresponds to Day 120 in Figure 15). The solar-time precession rate of Polar BEAR's orbit is represented by the slope of the bands. The solid lines with slightly greater slope outline the bands of HiLat passes above 30°, assuming that the two satellites are in the same local-time plane at the beginning of the epoch.

A key point illustrated by Figure 15 is that the slip rate between the two orbits is very small. The current precession rate for HiLat is greater (more negative) than that for Polar BEAR's nominal orbit by 18 sec/day. It is planned tentatively to inject Polar BEAR into a local-time plane one to two hours earlier than HiLat's after its launch sometime in the fourth quarter of 1986. Thereafter, Polar BEAR will move slowly toward time-of-day synchronism with HiLat, the condition illustrated at the beginning of Figure 15.

In the foregoing plan, coordinated observations employing the two satellites could begin immediately after Polar BEAR becomes operational and last for many months as they precess to, through, *and away* from the situation depicted in Figure 15. In a typical 30-day period during the epoch illustrated there, 143 Polar BEAR passes will reach a maximum elevation of at least 30°, and 118 HiLat passes will do so. During these passes, the satellites will be above 10° elevation for totals of 29.2 and 20.8 hours, respectively. Forty-two pairs of these will overlap in time, with a total overlap duration of 3.9 hours, and there will be 97 pairs in which such passes occur within 15 min of one another.

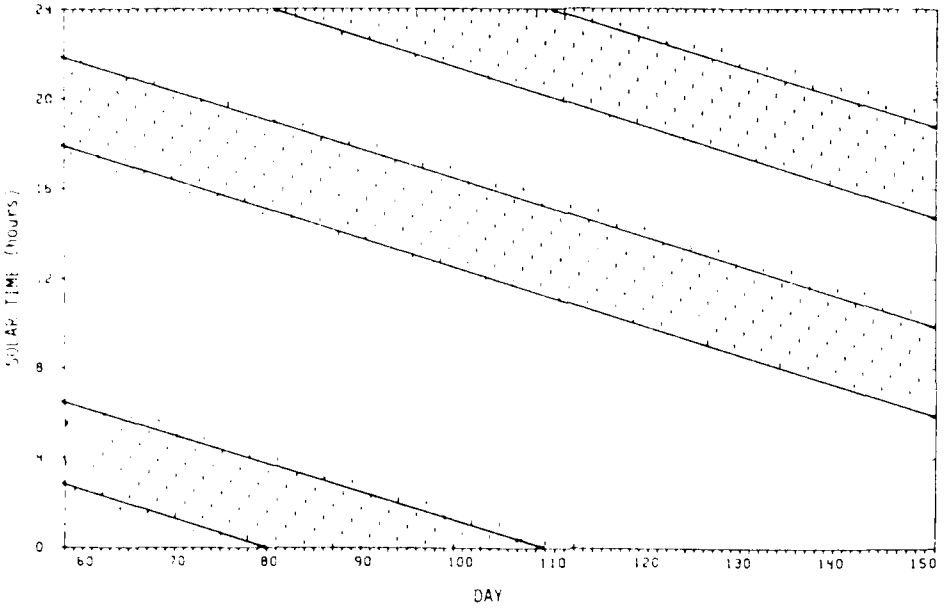

Figure 15. Pass times over Sondre Stromfjord during a representative calendar quarter. Short vertical dashes indicate Polar BEAR times above 10° elevation during individual passes with maximum elevations of at least 30°. Solid lines outline corresponding pass-time bands for what assuming that the two satellites are in the same local-time plane at the beginning of the epoch. Illustrating solar-time precession of the two orbital planes and the very small difference between their rates. (Supplied by R. Livingston, SRI.)

SECTION 6

DATA COLLECTION, PROCESSING, AND DISTRIBUTION

6.1 THE RECEIVING STATIONS.

The stations planned for receiving beacon and telemetry data from Polar BEAR and HiLat are those illustrated in Figure 1. The stations appear as stars also on Figure 16, which shows the slightly expanded coverage available at one of them, Sondre Stromfjord (SS), with Polar BEAR's increased altitude. The solid and broken circles again show, respectively, beacon and *in-situ* (magnetometer) coverage above 10° elevation from the station.

A likely routine operation is to record passes reaching a maximum elevation of at least 30° at the station. The area from which images could be recorded in such routine operation at a given station would be set by AIRS sweeps mainly during ascending and descending passes to the east and west of the station that just reach this elevation. The six-sided irregular boundary in Figure 16 roughly outlines that area for SS, set by the portions of such passes above 10° elevation and, in the south, by the 10° elevation circle itself (the effective boundary for nearly overhead passes). Combining images from all the stations gives extensive coverage of the northern auroral oval and polar cap, especially in the western hemisphere.

The imaging area indicated in Figure 16 is not that accessible on a single pass, but rather the total area imageable from all passes likely to be recorded routinely at SS. Figure 17 demonstrates the utility of multi-station operation for imaging, employing a pass particularly suited for obtaining a nearly complete quasi-snapshot (i.e., a composite image generated over a period of about 25 min) of the aurora and of the polar and sub-auroral airglow in the northern hemisphere (in the region enclosed by the quasi-rectangle). The trajectory illustrated passes nearly overhead at Bellevue, the north geomagnetic pole (center of plot), and Tromso and reaches maximum elevations of 50°, 28°, and 22° at Inuvik, Churchill, and SS, respectively.

Simply by adding such cases to the pass lists at SS and Churchill, nearly complete quasi-snapshots will be attainable with AIRS. Such operation will be especially informative when Polar BEAR is near the noon/midnight plane, when the auroral oval and polar cap will be shifted either toward (away from) or away from (toward) Tromso (Bellevue) at the appropriate universal time. Unfortunately, the

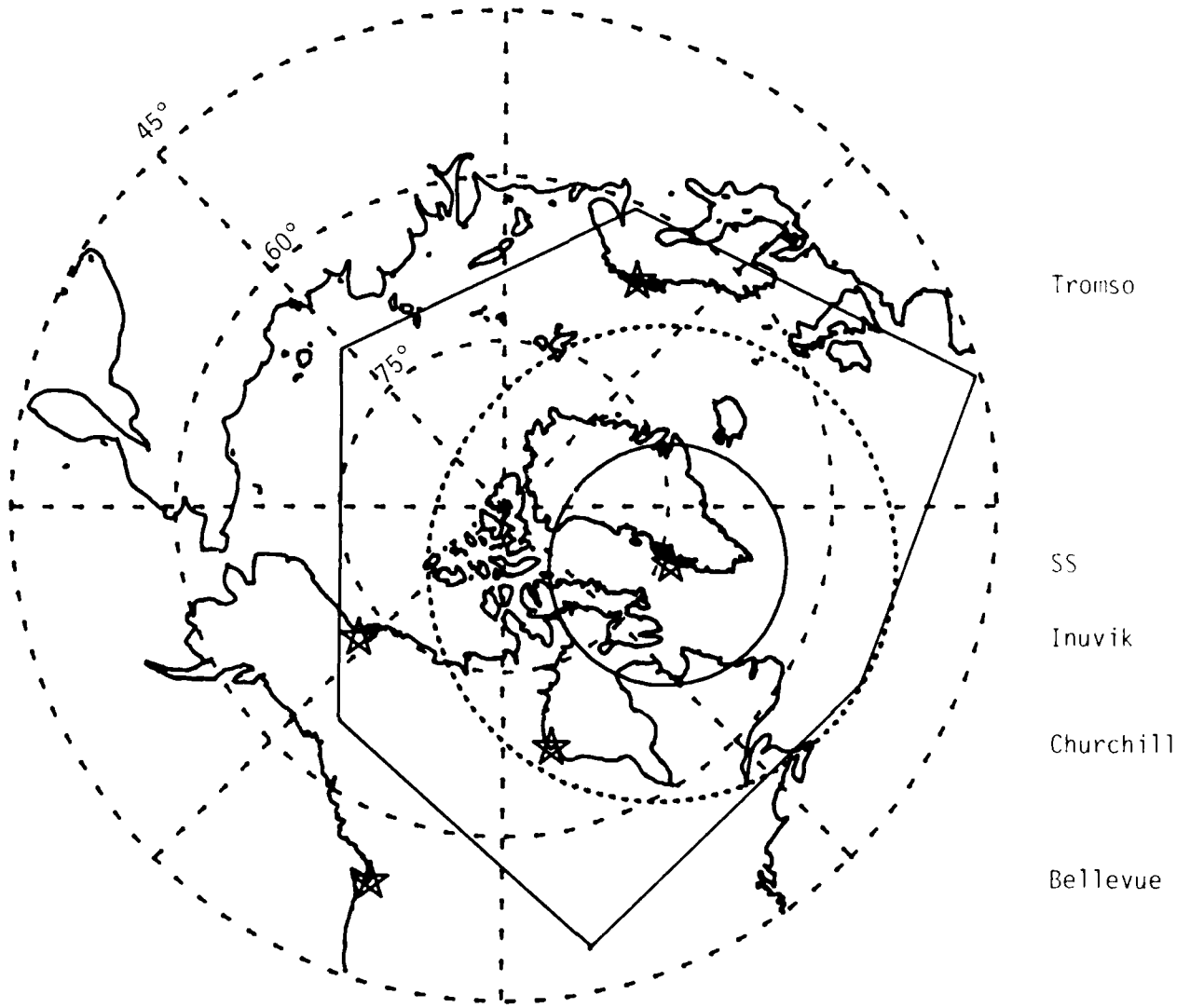

Figure 16. Polar BEAR coverage from the receiving station at Sondre Stromfjord, Greenland (SS). Solid and broken circles about the station show coverage above 10° elevation for beacon and magnetometer, respectively. Six-sided figure is approximate boundary of area imageable during passes reaching at least 30° elevation at SS. Other Polar BEAR stations, identified by stars, are Tromso, Norway; Inuvik, Northwest Territories; Churchill, Manitoba; and Bellevue, Washington. Inuvik has operated only sporadically for HiLat; its status and that of Churchill are not totally clear for the duration of Polar BEAR.

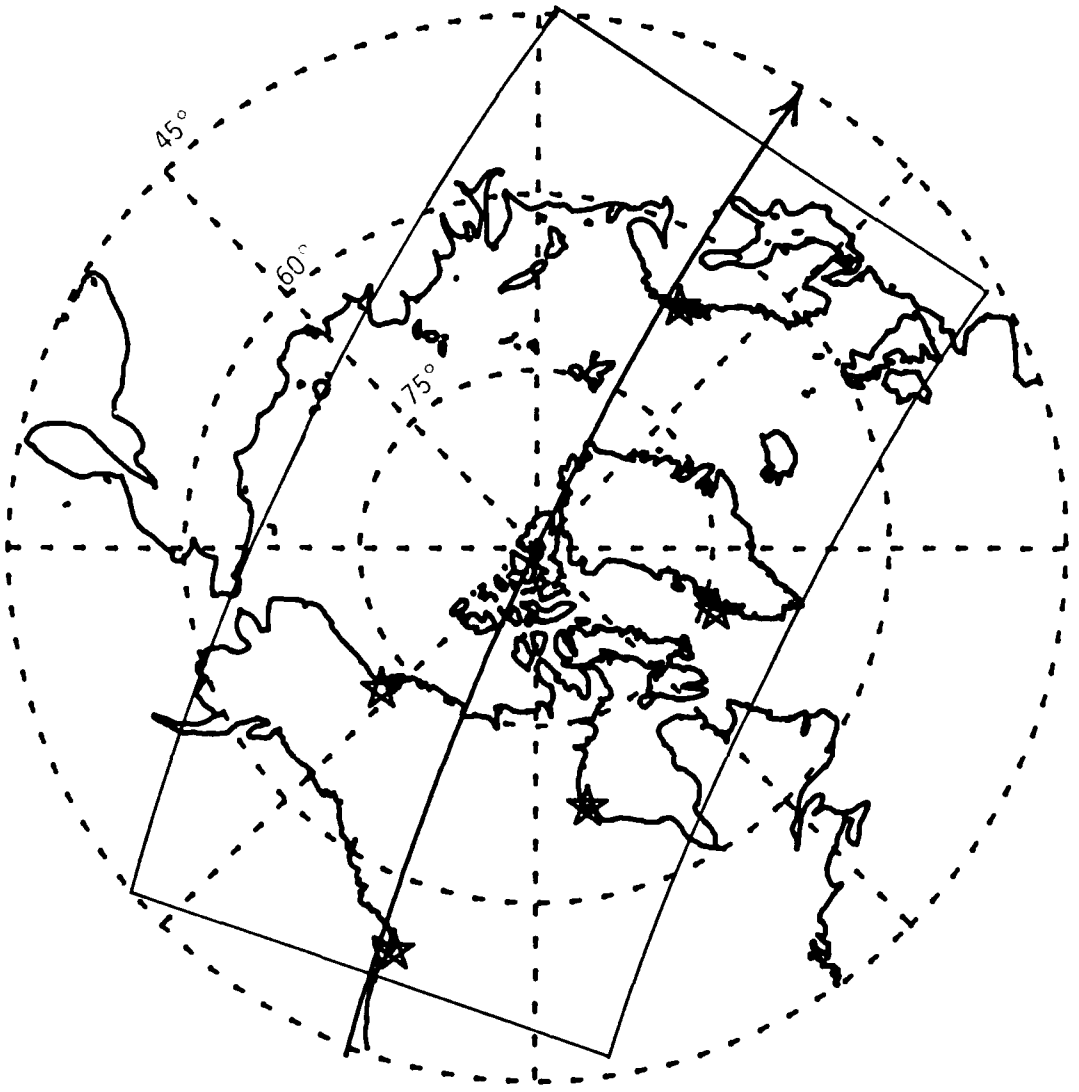

Figure 17. Illustrating the area (quasi-rectangle) in which a quasi-snapshot (combined image generated over a period of about 25 min) of the auroral oval and the polar and subauroral airglow will be attainable by combining AIRS data from multiple Polar BEAR stations.

station at Inuvik has operated only sporadically for HiLat, and its status and that of Churchill are not totally clear for the duration of Polar BEAR. Snapshots such as that illustrated in Figure 17 can be obtained without Inuvik, however, and only a small gap would occur from loss of Churchill.

An objective of Polar BEAR operation at the high-latitude receiving stations will be to maximize coincident observations between HiLat and Polar BEAR. Because of transmission licensing restrictions, the beacons on the two satellites will transmit at the same frequencies. Unless steps were taken to avoid it, mutual interference between the two would occur on about 20% of all passes, primarily because the beams of the VHF and UHF receiving antennas are rather broad. The quad-helix antennas presently used at L Band for HiLat produce narrower main lobes (about 10° full width at the half-power points) but also significant side lobes (about four dB lower than the main lobe) that extend out to ±45°.

The first step to be taken to reduce mutual interference is to replace the existing HiLat UHF and L-band antennas, which share common steerable flat ground screens, with UHF/L-band feeds in eight-foot steerable dishes, thus increasing gain and reducing side lobes. At L-band, the dishes will provide 26 dB of gain and produce full beamwidths of 14° between half-power points and 24° between first nulls. AT UHF, the corresponding parameters are 16 dB, 44°, and 70°. At SS and Tromso, these antennas will be used for reception of beacon and telemetry data from either HiLat or Polar BEAR when only one satellite is in the sky. At VHF, fixed antennas with upward-directed broad beams will continue to be used.

The main solution to the problem of mutual interference is that the Polar BEAR Beacon has been provided with an L-band-only operating mode, commandable from the ground. It will be used in conjunction with L-band-only receivers, and the second dishes, being added at SS and Tromso. When both satellites are in the sky, the full complement of data available from HiLat, including multi-frequency beacon data, will be collected using the existing receivers, and Polar BEAR will operate in its L-band-only mode to provide magnetometer data and AIRS images via the L-band-only receivers. Only in rare instances of nearly exact spatial and temporal coincidence between the two satellites should mutual interference be debilitating.

The receiving stations at Churchill, Bellevue, and Inuvik will remain configured essentially as they have been for HiLat. One exception is that attempts will be made to decrease the strength of L-band side lobes on the antenna at Bellevue. Since tha receiver, Rover, is to remain transportable to remote loca-

tions, there are practical limitations to the size, weight, and complexity of its antenna system. It employs the same L-band quad-helix and UHF single helix used at SS and Tromso, mounted on a common, steerable ground plane. Unlike that at the other stations, the same ground screen is used to house a VHF helix, thus providing a single, steerable antenna system for all frequencies.

Single-receiver operation at Bellevue will attempt to record all passes of both satellites that reach 30° elevation, when scheduling permits. When conflicts arise, Polar BEAR will be given priority if it is in its all-experiment mode. When Polar BEAR is in its L-band-only mode, priority will be given to HiLat so as to maximize collection of beacon data. Priority when Rover is on field excursions will depend upon the specific objective of the excursion, Polar BEAR likely being the priority satellite on most field trips.

In full operation, a HiLat/Polar BEAR receiver performs several functions. First, it receives, amplifies, and coherently detects the beacon signals, outputting the baseband in-phase and quadrature (I and Q) components of the scintillating VHF and UHF signals, employing a phase reference derived from the L-band signal. At the fixed stations, I and Q are recorded also from two UHF antennas spaced several hundred meters from the main antenna on orthogonal baselines for studying the spatial statistics of scintillation and the irregularities that cause it. Rover also can perform spaced receiver observations, but such measurements are not made when it is at Bellevue.

To obtain its phase reference, the receiver's L-band section contains a resynchronizing loop for reconstituting the L-band carrier suppressed by the BPSK data modulation. The phase of the reconstituted carrier is used to lock the entire receiver to the beacon's basic oscillator, with the frequency-differential effects of geometrical doppler automatically removed. The amplitude of the reconstituted carrier is recorded as a measure of L-band scintillation, which however usually is not strong enough in the ambient high-latitude environment to be of interest. Finally, the system demodulates the BPSK L-band signal and passes the bit stream from all non-beacon experiments to the station computer.

The computer performs the following functions. Prior to a satellite pass, it calculates look angles and doppler shift from orbit-ephemeris information received from NORAD. During the pass, the computed look angles are used for antenna steering, and the computed L-band doppler shift is used as a tuning aid for receiver lockup. The computer also controls data acquisition through an interface

and records it for post-pass processing. At the fixed stations, data are recorded on disk and processed into summary parameters for tape storage immediately after the pass. Rover's smaller computer records raw data directly on tape, and summary processing is performed on PDNW's mainframe computer after eight passes have been accumulated (typically, twice per week).

In addition to the antenna changes and addition of L-band-only receivers, the stations at SS and Tromso will be outfitted with larger (132-Mbyte) disks and faster CPUs (HP A900s) for their on-line computers, so that raw data from both HiLat and Polar BEAR may be recorded and then processed, simultaneously if necessary, into summary records. The summary data from all passes of both satellites and the raw data for some passes will be put on tape for permanent storage and analysis. All Rover data, both raw and summary-processed, from both satellites will be retained on tape.

6.2 DISSEMINATION OF DATA, EPHEMERIS INFORMATION, AND COMMANDS.

The data reduction performed in the field (at PDNW in the case of Rover) consists mainly of producing science-ready parameters. In addition, various kinds of geometry and observing-condition information are computed and placed on the summary tapes. The data tapes are distributed via the network shown in Figure 18. The five upper blocks represent the five HiLat/Polar BEAR receiving stations and the organizations responsible for their operation and data collection.

At the four fixed stations (Sondre Stromfjord, Tromso, Churchill, and Inuvik), raw data are reduced to summary form on site. Raw data from Rover flow through its home location, PDNW's laboratory at Bellevue, and are processed there; data from Inuvik flow through that receiver's parent organization, UWO. In all cases, raw and summary data are to flow to AFGL, the former for archiving and the latter for reproduction and distribution back to the participating organizations.

For antenna steering and receiver tuning for ready acquisition of signal, the satellite trajectory for each pass is computed at the receiving stations from ephemeris information provided by NORAD. Keplerian elements are distributed by NORAD over the network shown in Figure 19. Although a full data station normally is not operated by APL, it receives ephemeris information for observing the technical health of HiLat and Polar BEAR. The Naval Astronautics Group (NAG) employs the information for transmitting operating commands in a manner similar to its operational loading of commands into the TRANSIT Navy Navigation Satellites.

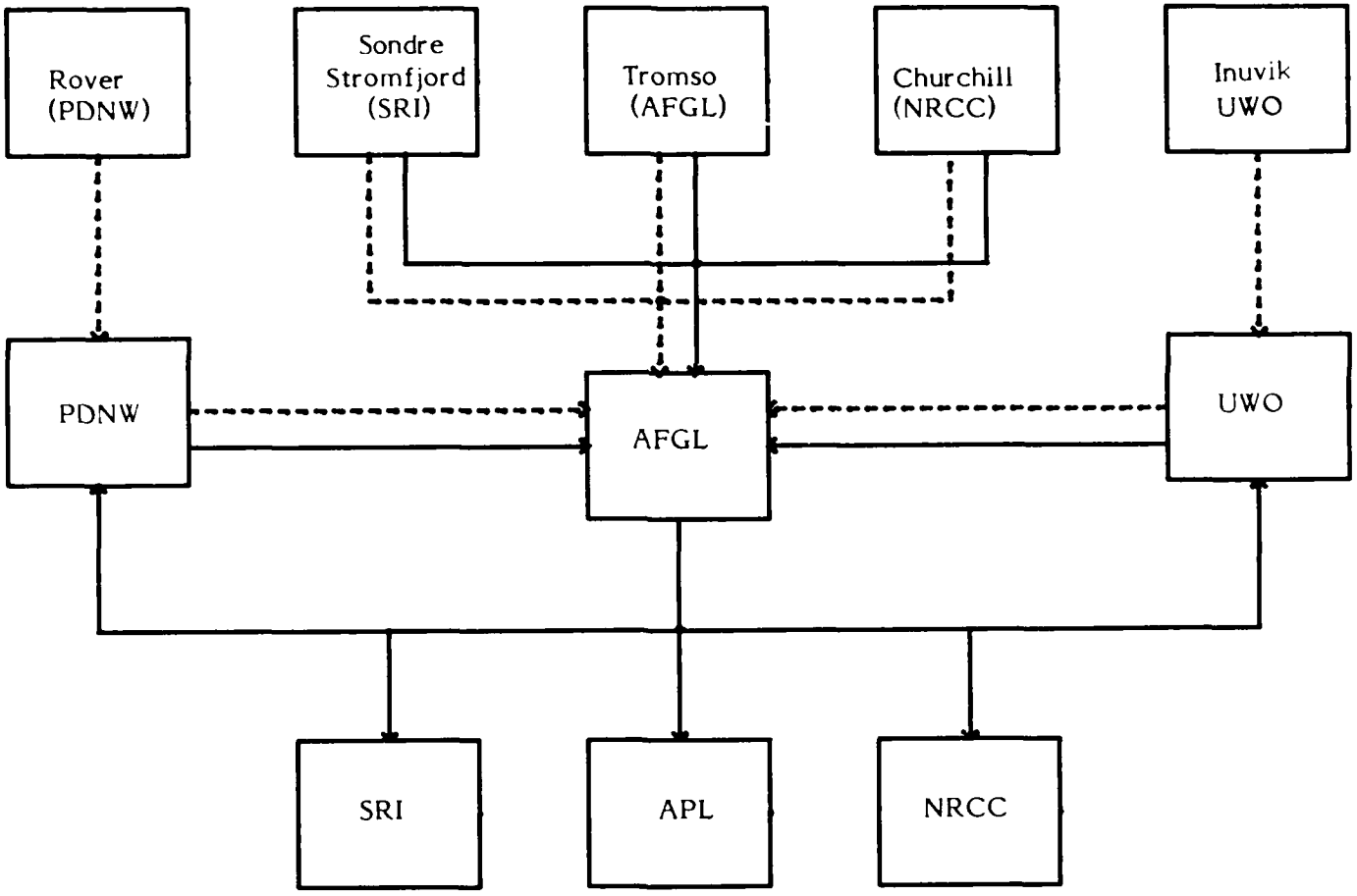

Figure 18. Data distribution network. Broken lines indicate flow of raw data for archiving, and solid lines represent flow of summary data for reproduction, followed by dissemination for analysis. (NRCC stands for National Research Council of Canada.)

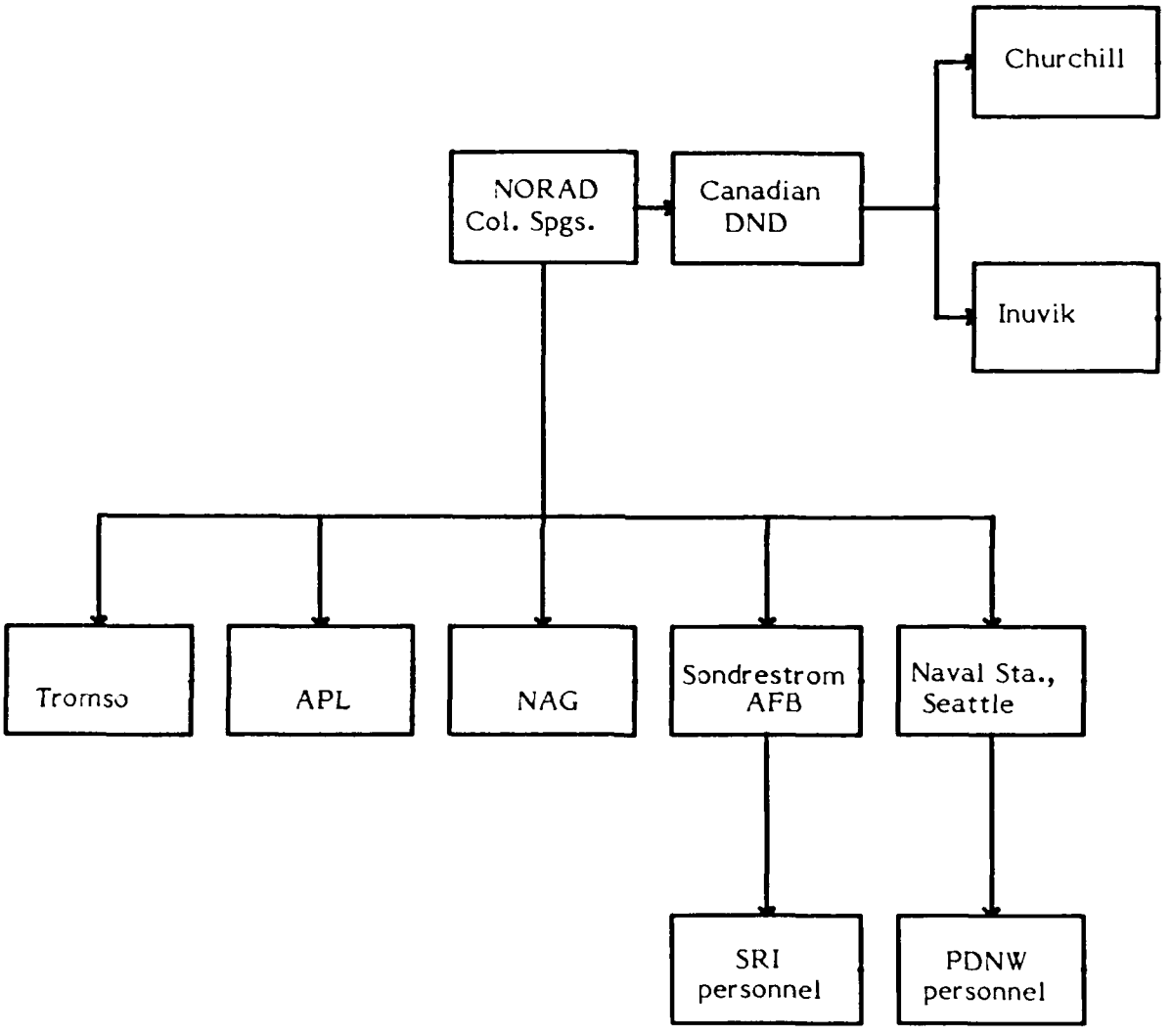

Figure 19. Ephemeris distribution network. (DND stands for Department of National Defense.)

Operating personnel from SRI and PDNW, respectively, hand carry ephemeris messages from local US military facilities to the Sondre Stromfjord station and to Rover when the latter is operating near Seattle. Other arrangements (e.g., commercial Telex) are made by PDNW when Rover is operating on a remote campaign, if necessary.

Unlike P76-5, which was able to operate its single payload (the Wideband Beacon) continuously, P83-1 and P87-1 have multiple payloads to support, and their power must be managed conservatively. For this purpose, they have timers on board, which permit payload operation only during one quarter of each orbit. The orbital phase of the operating period, which usually is over the earth's northern-most quadrant, can be shifted by command from the ground. The timer phase and instrument modes are set in advance by means of commands injected by NAG during passes over its network of stations, headquartered at Pt. Mugu, CA.

Mode requests from HiLat P.I.s normally are assembled by the Project Scientist at PDNW and passed to NAG for injection to the satellite. The same procedure will be followed for Polar BEAR, with additional requests from and deliberations with the organizations operating field sites being carried out by the Project Scientist for two-satellite operation. Command requests for technical management of each satellite normally come from its Project Engineer at APL. Only PDNW, APL, and DNA are authorized to issue command requests to NAG for HiLat/Polar BEAR ionospheric experiments and spacecraft operation.

SECTION 7

CONCLUSION

Three years after successful launch of P83-1, the HiLat/Polar BEAR Science Team views the increased understanding of high-latitude ionospheric dynamics and structuring that it has afforded with considerable satisfaction and some pride. As launch of its companion and successor, P87-1, approaches, the team looks forward, after a period of spacecraft stabilization, to a period of even more fruitful data collection and analysis. First and foremost, we await with very considerable anticipation the promise of AIRS images of the auroral oval and the polar and sub-auroral airglow. Secondly, we hope to glean firm insights into the workings of ionospheric plasma under the influence of high-latitude drivers as the new solar activity cycle begins to rise from its initial quiescence toward its full range of dynamism.

Given continued health of HiLat's retarding-potential analyzer and ion drift meter and continuation of the flawless performance so far turned in by its energetic electron spectrometer, addition of Polar BEAR's healthy magnetometer and AIRS' unique synoptic capabilities should contribute substantially to understanding the source mechanisms and evolution of the irregularities that produce scintillation of the signals received from the multi-frequency beacons carried by both satellites. This understanding, no doubt, will continue to be enhanced by contributions from other data sources. For example, AFGL's extensive instrumentation, including ground-based and airborne imaging, of the polar cap may be expected to continue making significant contributions, as may coherent and incoherent backscatter radars located for collaborative observations with HiLat and Polar BEAR.

Finally, interpretation, synthesis, and application of HiLat/Polar BEAR results will be facilitated greatly by the continued participation of plasma theorists and numericists from NRL and its contractors and by systems specialists and other researchers from MRC and Berkeley Research Associates. The resources and scientific leadership being made available by DNA to the Science Team continue to offer its members exciting opportunities for advancing the understanding of plasma-density irregularities, their development, and their effects on radio-frequency and optical systems.

SECTION 8

LIST OF REFERENCES

Basu, Su., S. Basu, C. Senior, D. Weimer, E. Nielsen, and P.F. Fougere (1986), "Velocity Shears and Sub-Km Scale Irregularities in the Nighttime Auroral F-Region," Geophys. Res. Ltrs., 13 (2), 101-104.

Buchau, J., E.J. Weber, H.C. Carlson, J.G. Moore, B.W. Reinisch, and R.C. Livingston (1984), "Ionospheric Structures in the Polar Cap and Their Relation to Satellite Scintillation," presented at the IES Symposium, 1-3 May, Alexandria, VA.

Burns, A.A. and E.J. Fremouw (1970), "A Real-Time Correction Technique for Transionospheric Ranging Error," IEEE Trans. on Antennas and Propagation," AP-18, 785-790.

Bythrow, P.F. (1986), "Field-aligned Currents, Velocity Shear, and Scintillation in the Cusp Region," Minutes of HiLat Science Team Meeting held 1 & 2 April, ed. Fremouw, Physical Dynamics Northwest Division, Bellevue, WA.

Bythrow, P.F., T.A. Potemra, W.B. Hanson, L.J. Zanetti, C.-I. Meng, R.E. Huffman, F.J. Rich, and D.A. Hardy (1984), "Earthward Directed High-Density Birkeland Currents Observed by HiLat," J. Geophys. Res., 89 (A10), 9114-9118.

Chandra, S., and E.I. Reed (1975), "Remote Sensing of the Ionospheric F Layer by Use of O I 6300-A and O I 1356-A Observations," J. Geophys. Res., 80 (16), 2327-2332.

Fedder, J.A., J.G. Lyon, and M.J. Keskinen (1986), "3D MHD Global Magnetospheric Simulations," Minutes of HiLat Science Team Meeting held 1 & 2 April, ed. Fremouw, Physical Dynamics Northwest Division, Bellevue, WA.

Fremouw, E.J. (1980), "Letter to H. Carl Fitz dated 5 June 1980.

Fremouw, E.J. (1981), "A Proposed Satellite-Borne Experiment for Describing and Understanding High-Latitude Plasma Structures," Proposal No. PD-NW-81-260P, Physical Dynamics, Inc., Bellevue, WA.

Fremouw, E.J. (1983), "HiLat: A Pre-Launch Overview," DNA-TR-81-276, Defense Nuclear Agency, Washington, DC.

Fremouw, E.J. (1985), "Recent HiLat Results," paper given at AGARD Symposium on Propagation Effects of Military Systems in the High Latitude Region, 3-7 June, Fairbanks, AK.

Fremouw, E.J., H.C. Carlson, T.A. Potemra, P.F. Bythrow, C.L. Rino, J.F. Vickrey, R.L. Livingston, R.E. Huffman, C.-I. Meng, D.A. Hardy, F.J. Rich, R.A. Heelis, W.B. Hanson, and L.A. Wittwer (1985), "The HiLat Satellite Mission," Rad. Sci., 20 (3), 416-424.

Fremouw, E.J., R.L. Leadabrand, R.C. Livingston, M.D. Cousins, C.L. Rino, B.C. Fair, and R.A. Long (1978), "Early Results from the DNA Wideband Satellite - Complex-Signal Scintillation," Radio Science, 13(1), 167-187.

Fremouw, E.J., C.L. Rino, R.C. Livingston, and M.C. Cousins (1977), "A Persistent Subauroral Scintillation Enhancement Observed in Alaska," Geophys. Res. Ltrs., 4 (11), 539.

HiLat Science Team (1984), "The DNA HiLat Satellite Mission," paper given at the IES Symposium, 1-3 May, Alexandria, VA.

Huffman, R.E., F.J. LeBlanc, J.C. Larrabee, and D.E. Paulsen (1980), "Satellite Vacuum Ultraviolet Airglow and Auroral Observations," J. Geophys. Res., 85 A5, 2201-2215.

Huffman, R.E. and C.-I. Meng (1984), "Ultraviolet Imaging of Sunlit Auroras from HiLat," Johns Hopkins APL Technical Digest, 5 (2), 138-142.

Ossakow, S.L. and P.K. Chaturvedi (1979), "Current Convective Instability in the Diffuse Aurora," Geophys. Res. Ltrs., 6, 332.

Rino, C.L. (1979), "A Power Law Phase Screen Model for Ionospheric Scintillation: 1. Weak Scatter," Rad. Sci., 14 (6), 1135.

Rino, C.L. (1985), "Spectral Characteristics, Theory & Experiment," Minutes of HiLat Science Team Meeting held 8 & 9 May, ed. Fremouw, Physical Dynamics Northwest Division, Bellevue, WA.

Rino, C.L., E.J. Fremouw, R.C. Livingston, M.D. Cousins, and B.S. Fair (1977), "Wideband Satellite Observations," DNA 4399F, Defense Nuclear Agency, Washington, DC.

Rino, C.L., R.C. Livingston, and S.J. Matthews (1978), "Evidence for Sheetlike Auroral Ionospheric Irregularities," Geophys. Res. Ltrs., 5 (12), 1039.

Schenkel, F.W., B.S. Ogorzalek, J.C. Larrabee, F.J. LeBlanc, and R.E. Huffman (1985), "Ultraviolet Daytime Auroral and Ionospheric Imaging from Space," Applied Optics, 24 (20), 3395-3405.

Zanetti, L.J. and T.A. Potemra (1982), "Correlated Birkeland Current Signatures from the Triad and MAGSAT Magnetic Field Data," Geophys. Res. Ltrs., 9 (4), 349-352.

DISTRIBUTION LIST

DEPARTMENT OF DEFENSE

DEFENSE INTELLIGENCE AGENCY
ATTN: RTS-2B

DEFENSE NUCLEAR AGENCY
ATTN: NATF
ATTN: NAWE
3 CYS ATTN: RAAE
ATTN: RAAE K SCHWARTZ
ATTN: RAAE P LUNN
ATTN: RAAE T WALSH
ATTN: RAEE
ATTN: STNA
4 CYS ATTN: STTI-CA

DEFENSE TECHNICAL INFORMATION CENTER
12 CYS ATTN: DD

FIELD COMMAND DNA DET 2
LAWRENCE LIVERMORE NATIONAL LAB
ATTN: FC 1

DEPARTMENT OF THE NAVY

NAVAL RESEARCH LABORATORY
ATTN: CODE 4180 J GOODMAN
ATTN: CODE 4700 S OSSAKOW
ATTN: CODE 4720 J DAVIS
ATTN: CODE 4732 B RIPIN
ATTN: CODE 4750 P RODRIGUEZ
ATTN: CODE 4780 J HUBA

DEPARTMENT OF THE AIR FORCE

AIR FORCE GEOPHYSICS LABORATORY
ATTN: CA A STAIR
ATTN: LID J RAMUSSEN
ATTN: LIS J BUCHAU
ATTN: LS
ATTN: LS R O'NIEL
ATTN: LSI H GARDINER
ATTN: LYD K CHAMPION

AIR FORCE SATELLITE CTRL FACILITY
ATTN: WE

AIR FORCE SPACE TECHNOLOGY CENTER
ATTN: XP

AIR FORCE TECHNICAL APPLICATIONS CTR
ATTN: TN

AIR FORCE WEAPONS LABORATORY, AFSC
ATTN: D H HILLAND
ATTN: NTN
ATTN: SUL

AIR FORCE WRIGHT AERONAUTICAL LAB/AAAD
ATTN: A JOHNSON
ATTN: W HUNT

DEPARTMENT OF ENERGY

UNIVERSITY OF CALIFORNIA
LOS ALAMOS NATIONAL LABORATORY
ATTN: D SAPPENFIELD
ATTN: D SIMONS
ATTN: J WOLCOTT
ATTN: MS J ZINN
ATTN: R JEFFRIES
ATTN: R W WHITAKER
ATTN: T KUNKLE

SANDIA NATIONAL LABORATORIES
ATTN: A D THORNBROUGH
ATTN: D DAHLGREN
ATTN: ORG 1231 T P WRIGHT
ATTN: ORG 314 W D BROWN
ATTN: ORG 332 R C BACKSTROM
ATTN: SPACE PROJECT DIV
ATTN: TECH LIB 3141 RPTS RCVG CLRK

OTHER GOVERNMENT

CENTRAL INTELLIGENCE AGENCY
ATTN: OSWR/NED
ATTN: OSWR/SSD FOR K FEUERPFEIL

DEPARTMENT OF DEFENSE CONTRACTORS

AEROSPACE CORP
ATTN: D OLSEN
ATTN: E RODRIGUEZ
ATTN: I GARFUNKEL
ATTN: J KLUCK
ATTN: J STRAUS
ATTN: K S CHO
ATTN: R SLAUGHTER
ATTN: T SALMI
ATTN: V JOSEPHSON

AUSTIN RESEARCH ASSOCIATES
ATTN: J THOMPSON

DEPT OF DEFENSE CONTRACTORS (CONTINUED)

CHARLES STARK DRAPER LAB, INC
ATTN: A TETEWSKI

EOS TECHNOLOGIES, INC
ATTN: B GABBARD
ATTN: W LELEVIER

INSTITUTE FOR DEFENSE ANALYSES
ATTN: E BAUER
ATTN: H WOLFHARD

JAYCOR
ATTN: J SPERLING

JOHNS HOPKINS UNIVERSITY
ATTN: C MENG
ATTN: J D PHILLIPS
ATTN: J NEWLAND
ATTN: K POTOCKI
ATTN: R STOKES
ATTN: T EVANS

KAMAN TEMPO
ATTN: B GAMBILL
ATTN: DASIAC
ATTN: R RUTHERFORD
ATTN: W MCNAMARA

KAMAN TEMPO
ATTN: DASIAC

M I T LINCOLN LAB
ATTN: D TOWLE
ATTN: I KUPIEC

MAXIM TECHNOLOGIES, INC
ATTN: J LEHMAN
ATTN: J MARSHALL
ATTN: J SO
ATTN: R MORGANSTERN

MISSION RESEARCH CORP
ATTN: B R MILNER
ATTN: C LAUER
ATTN: D ARCHER
ATTN: D KNEPP
ATTN: F FAJEN
ATTN: F GUIGLIANO
ATTN: G MCCARTOR
ATTN: R BIGONI
ATTN: R BOGUSCH
ATTN: R DANA
ATTN: R HENDRICK
ATTN: R KILB
ATTN: S GUTSCHE
ATTN: TECH LIBRARY

MITRE CORP
ATTN: A KYMMEL
ATTN: C CALLAHAN
ATTN: DR D RAMPTON
ATTN: M R DRESP

PACIFIC-SIERRA RESEARCH CORP
ATTN: E FIELD JR
ATTN: F THOMAS
ATTN: H BRODE, CHAIRMAN SAGE

PHYSICAL DYNAMICS, INC
2 CYS ATTN: E FREMOUW

PHYSICAL RESEARCH, INC
ATTN: R DELIBERIS
ATTN: T STEPHENS

PHYSICAL RESEARCH, INC
ATTN: J DEVORE
ATTN: J THOMPSON
ATTN: W SCHLUETER

R & D ASSOCIATES
ATTN: B LAMB
ATTN: B MOLLER
ATTN: C GREIFINGER
ATTN: F GILMORE
ATTN: H ORY
ATTN: M GANTSWEG
ATTN: M GROVER
ATTN: R TURCO
ATTN: W KARZAS

R & D ASSOCIATES
ATTN: B WEBSTER

R & D ASSOCIATES
ATTN: G GANONG

SCIENCE APPLICATIONS INTL CORP
ATTN: R LEADABRAND

SRI INTERNATIONAL
ATTN: D MCDANIEL
ATTN: W CHESNUT
ATTN: W JAYE

TECHNOLOGY INTERNATIONAL CORP
ATTN: W BOQUIST

TELECOMMUNICATIONS SCIENCES ASSOCIATES
ATTN: R BUCKNER

TOYON RESEARCH CORP
ATTN: J GARBARINO
ATTN: J ISE

VISIDYNE, INC
ATTN: J CARPENTER

END

3-87

DTIC